the plant journal

SEB SOCIETY FOR EXPERIMENTAL BIOLOGY

The Plant Journal (2024) **117,** 1413–1431 doi: 10.1111/tpj.16571

Constitutive expression of apple *endo-POLYGALACTURONASE1* in fruit induces early maturation, alters skin structure and accelerates softening

Kularajathevan Gunaseelan[1,†], Roswitha Schröder[1,†], Ria Rebstock[1], Annu S. Ninan[1], Cecilia Deng[1], Bishnu P. Khanal[2], Laurie Favre[3], Sumathi Tomes[1], Monica A. Dragulescu[1], Erin M. O'Donoghue[3], Ian C. Hallett[1], Robert J. Schaffer[4], Moritz Knoche[2], David A. Brummell[3] and Ross G. Atkinson[1,*]

[1]*The New Zealand Institute for Plant and Food Research Limited (Plant and Food Research), Mount Albert Research Centre, Private Bag 92169, Auckland 1142, New Zealand,*

[2]*Institute for Horticultural Production Systems, Leibniz-University Hannover, Herrenhäuser Straβe 2, 30419 Hannover, Germany,*

[3]*Plant and Food Research, Private Bag 11600, Palmerston North 4442, New Zealand, and*

[4]*Plant and Food Research, 55 Old Mill Rd, Motueka, 7198, New Zealand*

Received 6 June 2023; revised 25 October 2023; accepted 20 November 2023; published online 1 December 2023.
*For correspondence (e-mail ross.atkinson@plantandfood.co.nz).
†These authors contributed equally to this work.

SUMMARY

During fruit ripening, polygalacturonases (PGs) are key contributors to the softening process in many species. Apple is a crisp fruit that normally exhibits only minor changes to cell walls and limited fruit softening. Here, we explore the effects of PG overexpression during fruit development using transgenic apple lines overexpressing the ripening-related *endo-POLYGALACTURONASE1* gene. *MdPG1*-overexpressing (PGox) fruit displayed early maturation/ripening with black seeds, conversion of starch to sugars and ethylene production occurring by 80 days after pollination (DAP). PGox fruit exhibited a striking, white-skinned phenotype that was evident from 60 DAP and most likely resulted from increased air spaces and separation of cells in the hypodermis due to degradation of the middle lamellae. Irregularities in the integrity of the epidermis and cuticle were also observed. By 120 DAP, PGox fruit cracked and showed lenticel-associated russeting. Increased cuticular permeability was associated with microcracks in the cuticle around lenticels and was correlated with reduced cortical firmness at all time points and extensive post-harvest water loss from the fruit, resulting in premature shrivelling. Transcriptomic analysis suggested that early maturation was associated with upregulation of genes involved in stress responses, and overexpression of *MdPG1* also altered the expression of genes involved in cell wall metabolism (e.g. β-galactosidase, MD15G1221000) and ethylene biosynthesis (e.g. ACC synthase, MD14G1111500). The results show that upregulation of PG not only has dramatic effects on the structure of the fruit outer cell layers, indirectly affecting water status and turgor, but also has unexpected consequences for fruit development.

Keywords: cell separation, cell wall, *Malus domestica*, pectin, transpiration, transcriptomic analysis.

INTRODUCTION

The primary cell walls of fruit are composed of cellulose microfibrils embedded in an amorphous matrix of pectins, hemicelluloses and structural glycoproteins. Pectins are rich in galacturonic acid (GalA), and form supramolecules composed of four domains (Anderson & Kieber, 2020), with the most common being homogalacturonan (HG) and rhamnogalacturonan-I (RG-I). These two domains make up the middle lamella, the structure outside the primary wall that is responsible for effecting cell-to-cell adhesion (Zamil & Geitmann, 2017). During fruit ripening, softening and textural change (combined with alterations to colour, aroma and flavour) attract animals to eat the fruit and disperse the seeds (Giovannoni, 2001). Fruit softening and textural change is a multi-factorial process that involves alterations to water status and turgor (Shackel et al., 1991; Wada et al., 2008) combined with extensive modifications to many of the cell wall polysaccharides that bring about a controlled disassembly of the wall structure and reduced intercellular adhesion (Brummell, 2006; Shi et al., 2023).

One of the largest changes occurring in ripening fruit is the solubilisation and depolymerisation of high molecular weight pectins. The side chains of RG-I are degraded, and HG, which is initially secreted to the wall in a highly methylesterified form, is partially de-methylesterified by pectin methylesterase (PME). This not only makes HG susceptible to depolymerisation by endo-polygalacturonase (PG) and pectate lyase (PL), but also allows the formation of ionic Ca^{2+} bonds between stretches of charged, de-methylesterified HG in adjacent molecules. Depolymerisation of HG reduces wall strength and intercellular adhesion, whilst the formation of Ca^{2+}-pectate gels both prevents PG and PL action and provides an important component of intercellular adhesion in ripe fruit (Brummell, 2006; Shi et al., 2023).

The regulation of expression of the corresponding genes in fruit differs, with *PME* being developmentally controlled, unlike ripening-related *PG* and *PL* genes. In tomato, *PME* mRNA abundance peaks in green fruit and then declines, whilst activity increases to a peak during early ripening (Brummell & Harpster, 2001). In contrast, *PG* and *PL* mRNA abundance and activity increase during ripening. Genomic and transgenic studies have found that the mechanism of HG depolymerisation varies between species, being largely mediated by PG in melting flesh peach, by PL in tomato, and by both PG and PL in strawberry (Brummell, 2020). This suggests that not all fruit achieve softening identically, with some species predominantly using PG, some PL, and some both. In climacteric species, experiments using *ACC oxidase*-suppressed fruit (and hence deficient in endogenous ethylene production) show that expression of ripening-related *PG* genes is controlled by ethylene. In tomato, ripening-related *SlPG2a* is induced by very low concentrations of ethylene, although translation lagged behind mRNA accumulation by several days (Sitrit & Bennett, 1998). In apple, expression of the ripening-related *MdPG1* is controlled by ethylene but, at least post-harvest, can also be induced by extended cold temperatures in the absence of ethylene (Tacken et al., 2010).

In apple, a crisp fruit with limited softening, PG activity is too low to measure unless extensive protein purification is carried out (Wu et al., 1993), and changes in HG molecular weight distribution during ripening are slight. Nevertheless, antisense suppression of the ripening-related *MdPG1* gene significantly reduced fruit softening and led to small changes in the molecular weight distribution of HG and chelator-soluble (middle lamella) pectin, and a reduced proportion of water-soluble (WS) pectin (Atkinson et al., 2012). Alteration to the expression of this single gene also dramatically reduced post-harvest water loss (Atkinson et al., 2012), a major contributor to the maintenance of consumer traits such as crispness and crunchiness. This suggests an unexpectedly direct linkage between cell wall pectin modification and the alterations to cuticle composition, structure and properties that accompany ripening (Reynoud et al., 2022).

In apple, control of water loss is largely due to the permeability properties of the cuticle, since mature fruit generally lack stomata (Veraverbeke et al., 2003a, 2003b). Stomata turn into lenticels, which are filled with a periderm (Khanal et al., 2020). Structurally, the cuticle consists of a matrix of the polyester cutin, upon which are impregnated various waxes (and sometimes phenolics) that form a hydrophobic layer which is elaborated both within, and deposited upon the outer epidermal cell wall, where it provides the main barrier to water loss (Martin & Rose, 2014). In apple, the contribution of the cuticle to the mechanical properties of the fruit skin is marginal (Khanal & Knoche, 2014). In contrast, in the tomato cultivar 'DFD', an altered cuticle allowed minimal transpirational water loss and provided enhanced biomechanical support that maintained fruit firmness over an extended period (Saladié et al., 2007). In some species, such as blueberry, water loss may be the largest contributor to post-harvest softening (Paniagua et al., 2013).

Transgenic plants are a powerful tool to determine gene function and effects on plant phenotype. Downregulation of PG and PL in fruit has shown the importance of these genes to fruit firmness and other fruit quality traits such as texture and storage life (Brummell et al., 2022). Overexpression of cell wall genes in leaves, roots and flowers (Atkinson et al., 2002; He et al., 2019; Ohara et al., 2021; Rui et al., 2017; Xiao et al., 2014) has allowed new roles in floral organ patterning, response to biotic stress and stomatal dynamics to be ascribed to PGs. However, stable overexpression of cell wall genes in fruit is more rarely reported. Overexpression of ripening-related cell wall genes encoding expansin, PL or xyloglucan endotransglycosylase/hydrolase (XTH) in tomato produced fruit that were softer than controls, but otherwise fruit developed relatively normally (Brummell et al., 1999; Chen et al., 2022; Han et al., 2016; Li et al., 2023). Here, we report the effects of overexpression of the *MdPG1* gene in developing apple fruit. Our results show that PG overexpression from early in fruit development has strong phenotypic effects, including accelerated fruit maturation/ripening, and changes to visual appearance, fruit firmness and post-harvest water loss. These effects can be linked to changes in intercellular connections, apple cell wall structure and skin permeability. Our results further highlight the importance of *MdPG1* to apple fruit softening (Atkinson et al., 2012; Costa et al., 2010; Longhi et al., 2013) and reveal new and unexpected developmental consequences of PG overexpression.

RESULTS

Phenotypic analysis of apple fruit overexpressing *MdPG1*

Twenty independent 'Royal Gala' transgenic lines were generated that constitutively overexpressed the apple *MdPG1* gene under the control of the CaMV 35S promoter. Since endogenous *MdPG1* expression is ripening-related and does not normally occur in vegetative tissues or

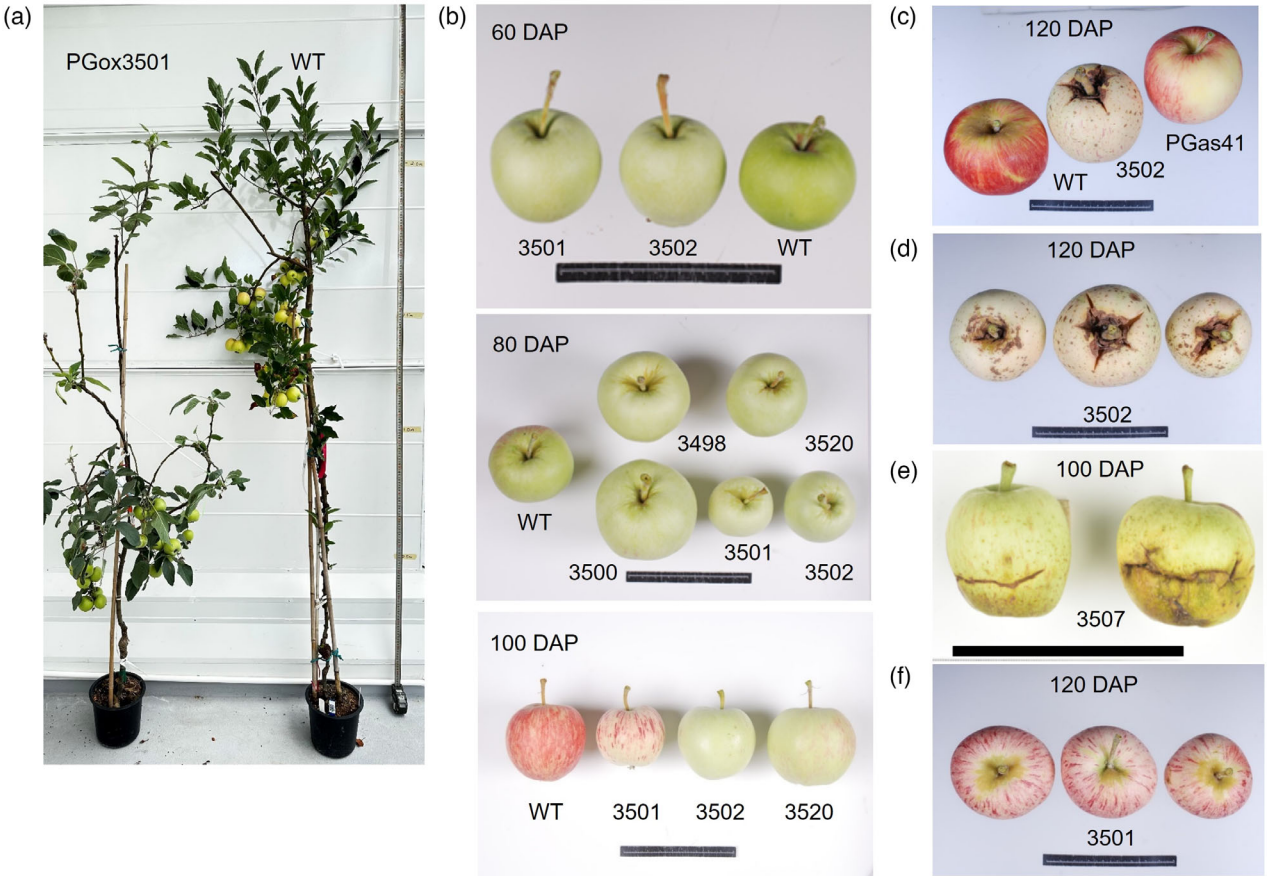

Figure 1. Phenotypes of transgenic PGox apple plants and fruit.
(a) Weak growth habit of PGox3501 compared with the stronger growth of a wildtype (WT) tree (height = approximately 2.5 m).
(b) Representative photographs of fruit from WT and PGox lines with white skin at 60, 80 and 100 days after pollination (DAP).
(c) Fruit size in WT, PGox3502 and a PG antisense line (PGas41) at 120 DAP.
(d) Russeting around lenticels and cracking observed in PGox3502.
(e) Fruit cracking in PGox3507.
(f) Red colour development on typical white skin in PGox3501. Scale bar in all fruit pictures = 9 cm.

unripe fruit, transgenic plantlets could be screened prior to fruit set by examining leaves. Initial screening of these PGox lines using leaves (Figure S1a) indicated that most of the lines showed the abscission and silver-leaf phenotypes previously observed (Atkinson et al., 2002). Biochemical and molecular analysis of the leaves of these plants also showed that multiple lines overexpressed the MdPG1 protein (Figure S1b) and *MdPG1* gene (Figure S1c).

The growth of the PGox apple plants in the containment glasshouse was greatly compromised compared with that of wildtype (WT) 'Royal Gala' (Figure 1a). PGox plants were highly sensitive to dehydration and to temperature variations. However, by careful management of the plants, multiple PGox lines flowered, and small numbers of fruit (<10) on each plant were obtained for further analysis. Fruit from multiple PGox lines showed a striking, white-skinned phenotype that was evident from 60 days after pollination (DAP) but became more pronounced at 80 and 100 DAP (Figure 1b). This result was confirmed by chromameter (LCH) measurements that indicated that the fruit of all PGox lines had higher 'L' values (indicating higher whiteness) compared with WT at all three sampling time points (Figure S1d).

There was considerable variation in the size of individual fruit from both WT and the PGox lines (Figure 1b, middle panel). However, on average, fruit size and weight in the PGox lines were typically lower when compared with WT (Figure 1c; Figure S2a). Lenticel-associated russeting was observed on the skin of some PGox lines (Figure 1d). Large cracks were observed in the fruit of some PGox lines (e.g. 3502, 3507, Figure 1d,e), but not in others (e.g. 3501, Figure 1f). Cracks were not observed in any lines at 60 days or 80 DAP but by 100 DAP most fruit from PGox lines 3502 and 3507 showed evidence of cracking. Lines with cracking were susceptible to post-harvest infection and could not be stored.

Red colour associated with anthocyanin production was observed in the fruit skin of WT and some PGox lines (e.g. PGox 3501, 3520) from 100 DAP (Figure 1b). The red

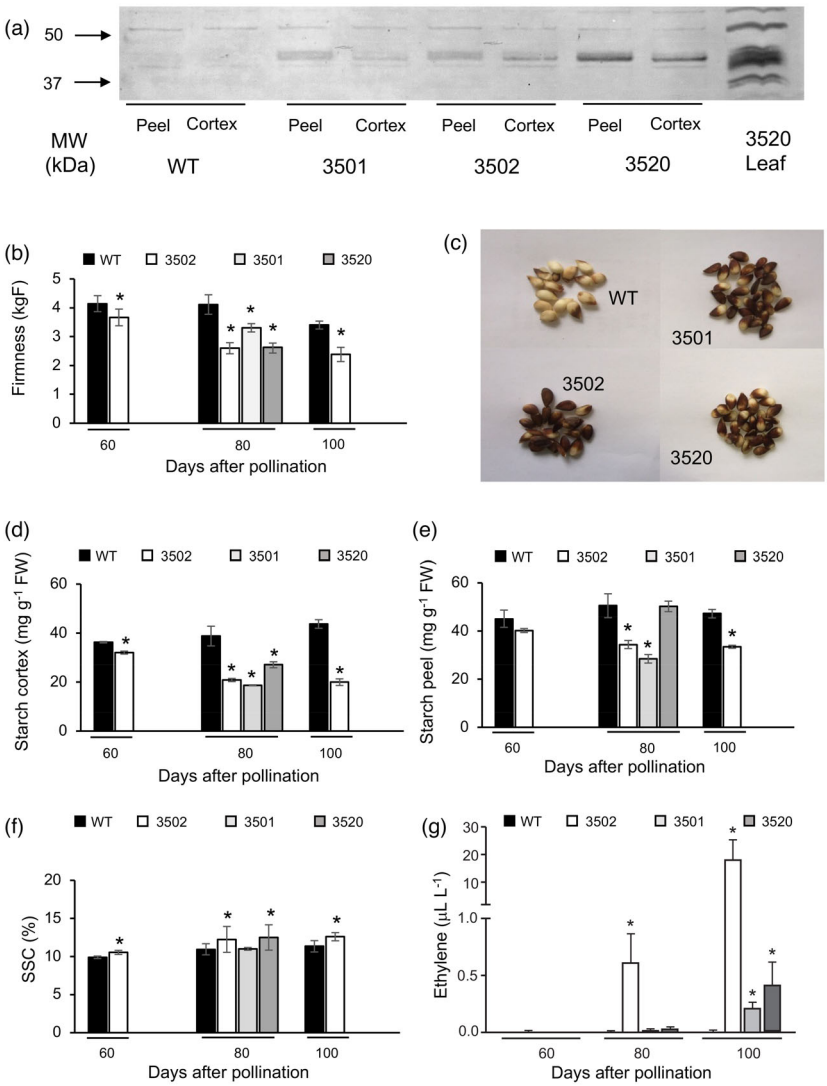

Figure 2. Biochemical and physiological characterisation of three selected PGox apple lines.
(a) Protein gel blot showing abundance of immunodetectable MdPG1 protein (expected size 45 kDa) in the peel and cortex of wildtype (WT) and PGox (3501, 3502, 3520) fruit at 80 days after pollination (DAP) and in PGox3520 leaf. MW = molecular weight marker in kDa (Precision Plus Protein Dual Color MW marker; Bio-Rad).
(b–g) Comparison of WT and PGox lines during fruit development.
(b) Cortex firmness.
(c) Seed coat colour at 80 DAP.
(d) Starch content in cortex.
(e) Starch content in peel.
(f) Soluble solids content (SSC).
(g) Ethylene production. Values are means ± SD of >5 fruit per time point over two seasons. Starch was quantified using three biological replicates per time point with two technical replicates each. * Indicates statistically different ($P < 0.05$) means between the WT and PGox at the same developmental stage.

colouration in these lines was observed overlying the white-skinned phenotype (Figure 1f). However, some PGox fruit produced little if any red colour (e.g. PGox 3502) even at 120 DAP (Figure 1d). Chromameter (LCH) measurements indicated that the 'H' values of PGox lines and WT lines were similar at 60 and 80 DAP (Figure S1d). At 100 DAP, the 'H' value in WT fruit decreased (indicating a decrease in green colouration and an increase in red). 'H' values also decreased at 100 DAP in PGox3501, but not in PGox3502. The intensity of red colour varied amongst fruit from the same line and from fruit obtained from the same tree in different years. This suggests that factors other than the transgene, for example light and other environmental conditions, are influencing the development of red colour.

Fruit from the PGox lines and the WT were harvested at 80 DAP and tested for cortical firmness (Figure S2b). All lines (except PGox3505 and 3518) showed a significant reduction in cortical firmness. Based on this screen, in combination with the biochemical and molecular analysis of leaves (Figure S1a–c), PGox lines 3501, 3502, 3507 and 3520 were macro-grafted onto 'M9' rootstocks to obtain more fruit for further analysis.

Biochemical and physiological characterisation of PGox lines

Three macro-grafted PGox lines with the strongest visible fruit phenotypes (3501, 3502 and 3520) were used for biochemical and physiological characterisation. Western blot analysis using an MdPG1-specific antibody on peel and cortex tissues harvested at 80 DAP indicated that all three lines overexpressed MdPG1 in both tissues, but more so in peel (Figure 2a). PGox3520 showed the most intense bands. No MdPG1 was detected in WT fruit tissue. Cortical firmness was significantly reduced in fruit at 80 DAP in all three PGox lines (Figure 2b). Cortical firmness was also measured in fruit from PGox3502 harvested at 60 and

100 DAP, and at both time points cortical firmness was reduced in the PGox line compared with that of the WT (Figure 2b).

In WT 'Royal Gala' grown under glasshouse conditions, fruit development is marked by the following changes. At approximately 110 DAP, seed colour changes from white to black. This seed colour change is a standard measure of fruit maturity in apple (Kingston, 1992). Following this, starch breakdown is initiated and there is an increase in soluble sugar content. At 135 DAP, fruit is typically harvested (Janssen et al., 2008) and ethylene-associated ripening starts. Concomitant with increasing ethylene production, fruit begin to soften and volatiles are produced (Schaffer et al., 2007). Seed extracted from fruit at 80 DAP suggested that maturation of PGox lines was accelerated compared with that of the controls. In WT lines, the seed coat at 80 DAP was white, whilst in PGox lines, the seeds were already brown (Figure 2c). Consistent with this observation, the starch content in the cortical tissue was lower in all three PGox lines at 80 DAP, and in PGox3502 at 60 and 100 DAP (Figure 2d). Starch content in the peel tissue was also significantly lower in PGox 3502 and 3501 than in the WT at 80 DAP (Figure 2e). Soluble solids contents were higher in the cortex of PGox3502 and 3520 at 80 DAP (Figure 2f). In PGox3502, increased soluble solids and reduced starch contents were observed as early as 60 DAP (Figure 2d–f).

A further marker of advanced maturity and ripening is the production of ethylene. No ethylene was detected in WT fruit from 60 to 100 DAP, whilst variable and low amounts (compared with that typically found in ethylene-treated 'Royal Gala' fruit [Yauk et al., 2015]) were observed in the PGox lines (Figure 2g). Extraction of chlorophyll from the peel of PGox lines and WT indicated that concentrations of chlorophyll were similar between WT and PGox at 80 and 100 DAP (Figure S2c). Concentrations of anthocyanin were also similar or slightly elevated in the peel of PGox fruit compared with WT (Figure S2d).

Structure and intercellular connections of the skin are changed during development

The structures of the fruit skin (consisting of the cuticle, epidermis and hypodermis) and the cortical cells immediately below were compared by histochemical staining during the development of WT and PGox3502 fruit from 60 to 100 DAP. Throughout this period, WT apples had a similar morphology (Figure 3a–c). Below a single layer of thin-walled epidermal cells was the hypodermal layer, comprising thick-walled, oval-shaped cells that were tightly packed and three to five cell layers deep. Below the hypodermis were the larger parenchyma cells of the cortex, which increased in size further from the skin. These cells were interspaced with air spaces, with the size and frequency of these air spaces increasing further into the cortex. PGox3502 skin had thinner cell walls and markedly more air spaces at all stages of development (Figures 3d–f). This was particularly evident within the hypodermis and cortical cells immediately below that. Large airspaces beneath the epidermis were found only in the PGox line, and their size and frequency increased during fruit development. The white-skinned phenotype of the PGox lines most likely resulted from additional light scattering due to separation of the epidermal layers from the hypodermis since the PGox lines were not lacking in chlorophyll or anthocyanins (Figure S2c,d). Variation in air space distribution within the same fruit and between fruit was most notable at 80 DAP, highlighting the non-uniform distribution of air spaces within individual fruit and the non-linear progression of air-space development in apples overexpressing PG. Cryo-SEM analysis of fractured frozen apple tissue from the WT and PGox3502 and 3501 at 120 DAP confirmed that the changes to intercellular adhesion and cell wall composition in the outer cell layers had a large effect on the internal structure of the fruit, with the presence of more and larger airspaces in the two PGox lines (Figure S4).

Immunolabelling of peel sections of WT fruit from 60 to 100 DAP indicated that epitopes of linearised arabinan (LM13) were detected only within the epidermis, with less frequent labelling occurring in the hypodermal cells at 100 DAP (Figure 3g–i). In sections from PGox3502 fruit, linearised arabinan epitopes were also localised only in the epidermis during early development, but more epitopes were present throughout the hypodermal cell walls at both 80 and 100 DAP (Figure 3j–l). Antibodies recognising branched arabinans (LM6) and the HG backbone with various degrees of methyl esterification (LM20, JIM5) did not show any difference between the WT and PGox3502 at the developmental stages tested.

Overexpression of *MdPG1* in apple leads to faster water loss from the fruit

Analysis of apple fruit surfaces by fluorescence microscopy revealed intact surfaces in the WT (Figure 4a), but numerous microcracks in the cuticle of the PGox line (Figure 4b). Many of these microcracks in PGox3502 occurred around lenticels. Cuticle thickness and morphology were otherwise similar between the WT and PGox3502 (Figure 4c,d).

PGox fruit showed excessive water loss when harvested at 120 DAP and kept at room temperature. The most extreme example was for PGox3502, where the fruit shrivelled and dried out within 4 weeks compared with the WT controls (Figure 4e). To study this phenotype in more detail, time courses of transpiration from excised skin segments (Figure 4f) and from whole fruit (Figure 4f inset) were compared for the WT and three PGox lines (3502, 3507, 3520). Fruit from a PG antisense line (PGas41) (Atkinson et al., 2012) were also included in the study as an additional control. Transpiration increased linearly with time on a whole-fruit basis and through excised skin segments,

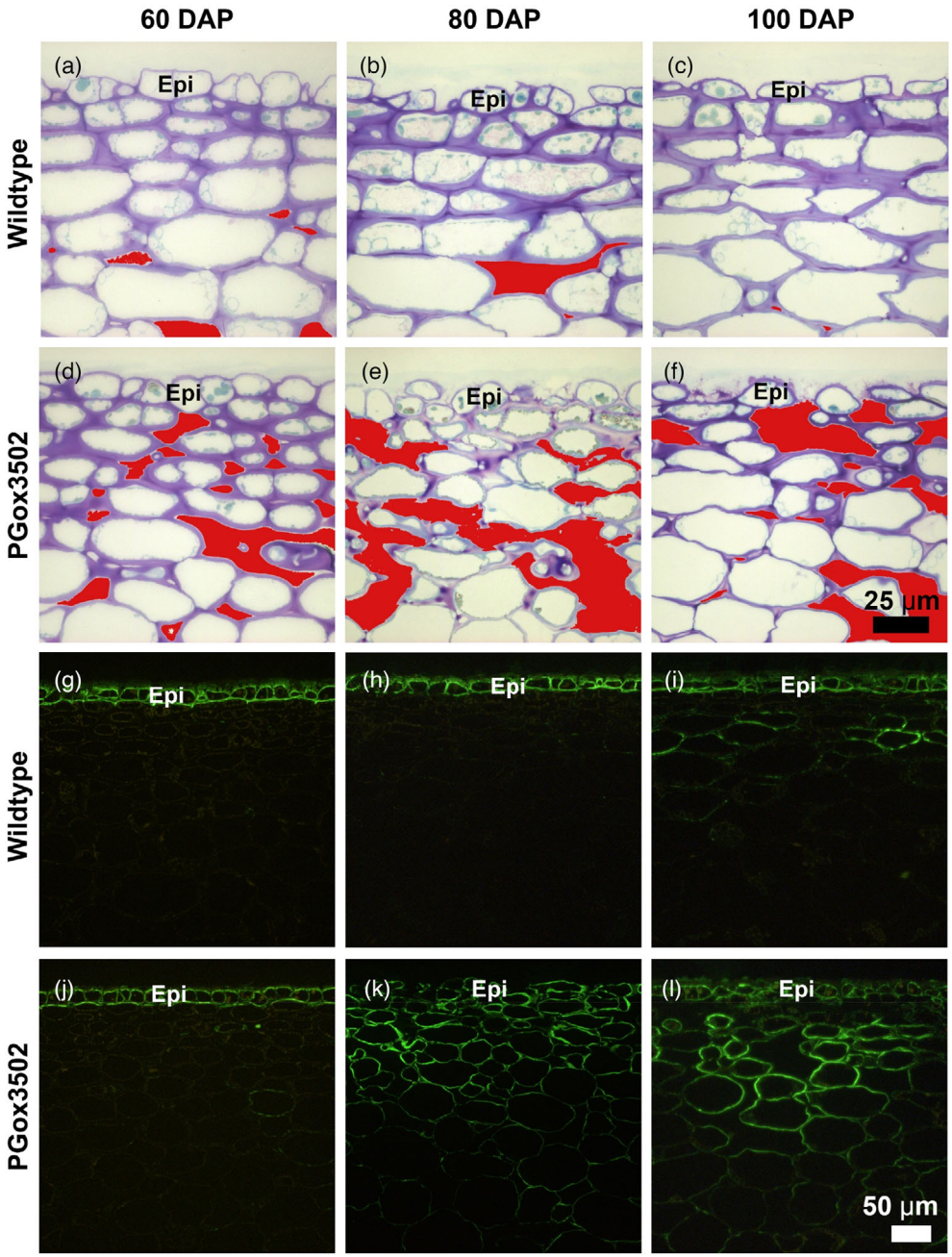

Figure 3. Structure of the apple fruit outer cell layers.
(a–f) Toluidine blue staining of wildtype and PGox3502 fruit harvested at 60, 80 and 100 days after pollination (DAP). Airspaces have been false-coloured red for comparison. The original images are presented in Figure S3a–f. Similar results were obtained for PGox3501 (Figure S3g–i). Scale is the same for all images.
(g–l) Immunolabelling of linear arabinan epitopes using LM13 antibody. Scale is the same for all images. Epi = epidermis/cuticle region.

indicating that the rates of transpiration remained constant. Probability plots revealed that the log-transformed permeances (P) of all lines were essentially normally distributed. There was no difference in the frequency distributions of the values for permeance for the PG antisense apples and the WT over this timescale. However, the distribution of the permeance of the PGox fruit was displaced and less steep, indicating a higher and more variable permeance value (Figure 4g, Table 1). Permeances of the PGox lines were significantly higher than those of the WT and the antisense line. There was no significant difference between PGox lines.

PGox fruit show altered pectin solubilisation and galactose loss

To investigate the effects of PG overexpression on the chemistry of fruit cell walls, extracts were prepared from

the WT and three PGox lines (3501, 3502, 3520) at 80 DAP, as well as from the WT and PGox3502 at 60 and 100 DAP. On a fresh weight (FW) basis, PGox fruit contained 13–34% less cell wall material (CWM) in peel tissue than the WT over development (Figure 5a). This was particularly pronounced at 80 DAP, when strong phenotypic differences had developed. The reduced amount of CWM was consistent with the altered appearance of the outer cell layers, which in the overexpression lines had thinner cell walls and were disorganised with spaces filled with fluid or air between cells (Figure 3). The yield of CWM from cortex tissue was not influenced by overexpression of PG (Figure 5b).

The largest effect of overexpression of *MdPG1* on fruit cell walls was on the amount of material in the WS extract (Figure 5c,d), an extract enriched in GalA and consisting predominantly of HG and RG-I (Table S1). In peel, PGox lines had a 45–60% greater amount of WS pectin at 80 DAP (Figure 5c), with a comparison between different DAPs using line PGox3502 suggesting that the greater amount relative to that of the WT decreased with advancing development. In the insoluble CWM remaining after extraction of the WS component, the contents of GalA were similar between WT and transgenic lines (Figure 5e,f). The partitioning of material between pectin-rich cell wall extracts (CDTA-, Na_2CO_3-soluble extracts) and cell wall residue was not influenced by overexpression of PG (Table S2). Polyuronide size distribution determined using size exclusion chromatography of water-, CDTA- and Na_2CO_3-soluble extracts derived from cell walls of both tissues was similar between WT and PGox lines (Figures S5–S7). Analysis of the sugar composition of all three of these soluble extracts showed that they were composed predominantly of arabinose, galactose and uronic acids (UA), indicating that they contained mainly HG and RG-I-type pectin (Table S1). The degree of methyl esterification of CWM and CDTA extracts of peel and cortex was also similar in WT and PGox lines (Figure S8).

To determine the effects of overexpression of *MdPG1* on cell wall RG-I, the neutral sugar composition of the insoluble CWM was examined. The arabinosyl content of peel and cortex cell walls was largely similar between PGox fruit and the WT (Figure 5g, h), suggesting only minor effects on cell wall arabinans. In contrast, the galactosyl content of insoluble CWM was lower in the peel and cortex cell walls of most PGox genotypes than in the WT (Figure 5i,j), indicating a substantial loss of RG-I galactans.

Oligogalacturonides from wildtype and PGox fruit

One hypothesis to account for the early maturation phenotype in PGox fruit is that the MdPG1 enzyme generates physiologically active oligogalacturonides (OGs, α-1,4-linked galacturonosyl residues) with a degree of polymerisation (DP) of 4–6 by hydrolysis of HG (Ma et al., 2016; Simpson et al., 1998). At 80 DAP, OGs of various sizes were present in the fruit cortex tissue of wildtype and three PGox lines, with slightly greater abundance in the DP 4–6 range (Figure 6a). However, at 60 DAP the size distribution of OGs was not greatly different in line 3502 from that in the WT (Figure 6b), when the white-skin phenotype was already apparent (Figure 1b). As the chronological age of the fruit increased, the OGs became more polydisperse, with fewer OGs in the putatively biologically active size range (Figure 6b–d).

Transcriptomic analysis of wildtype and PGox fruit peel

Transcriptomic profiles of PGox3502 and WT fruit peel samples (thinly pared shavings from the fruit surface, including some outer cortex) were compared to analyse differences in gene expression at 60, 80 and 100 DAP. The outer tissues of the fruit were selected since this is where the phenotype was most visible. Between 17 and 37 million reads were generated per library, with 82–86% overall mapping rate to the GDDH reference genome (Daccord et al., 2017). Principal component analysis (PCA) was used to observe the distribution of the samples in two-dimensional space (Figure 7a). The first component accounted for 65.2% of the variance, and samples were distributed according to chronological age, with samples moving to the left as age increased. The second component (13% of the variance) represented the transgene effect, separating the WT from PGox at each time point. Samples at 60 and 100 DAP showed good clustering within replicates, but more variation was observed in the 80 DAP samples, possibly due to the challenge of producing good replicates from small numbers of fruit.

Because of the tight clustering of replicates at 60 and 100 DAP, we focused on identification of differentially expressed genes (DEGs) between the WT and PGox samples at these two time points. At 60 DAP, 588 DEGs were identified and at 100 DAP, 466 DEGs were identified with a $>$ 4-fold difference (abs(logFC) $\geq$2 and adjusted *P*-value $<$0.05) between WT and PGox samples (Table S3). Eighty-one DEGs were shared between the two time points. About 80% of the DEGs identified at each time point were upregulated in the PGox line and only 20% downregulated. The most DEG (logFC $>$12) at both 60 and 100 DAP was the CaMV 35S-driven transgene *MdPG1* (Table 2, Table S3). Other cell wall genes that were differentially expressed in the PGox fruit included three β-galactosidases, two cellulose synthases, two pectin lyase-like superfamily proteins and three genes belonging to the PME inhibitor family. Genes involved in ethylene biosynthesis and action, such as ACC synthase, ACC oxidase and an ethylene response factor, were strongly upregulated as early as 60 DAP (Table 2).

A number of genes involved in responses to water and temperature stress were differentially regulated,

including two dehydrin genes (Table 2). However, the most striking observation was the upregulation at 60 DAP of a suite of genes encoding various heat shock proteins and a chaperonin. There was little change in the expression of the seven genes annotated as being involved in chlorophyll degradation (Table S3), consistent with the similar levels of chlorophyll found in the samples (Figure S2c). mRNA encoding the key anthocyanin regulating

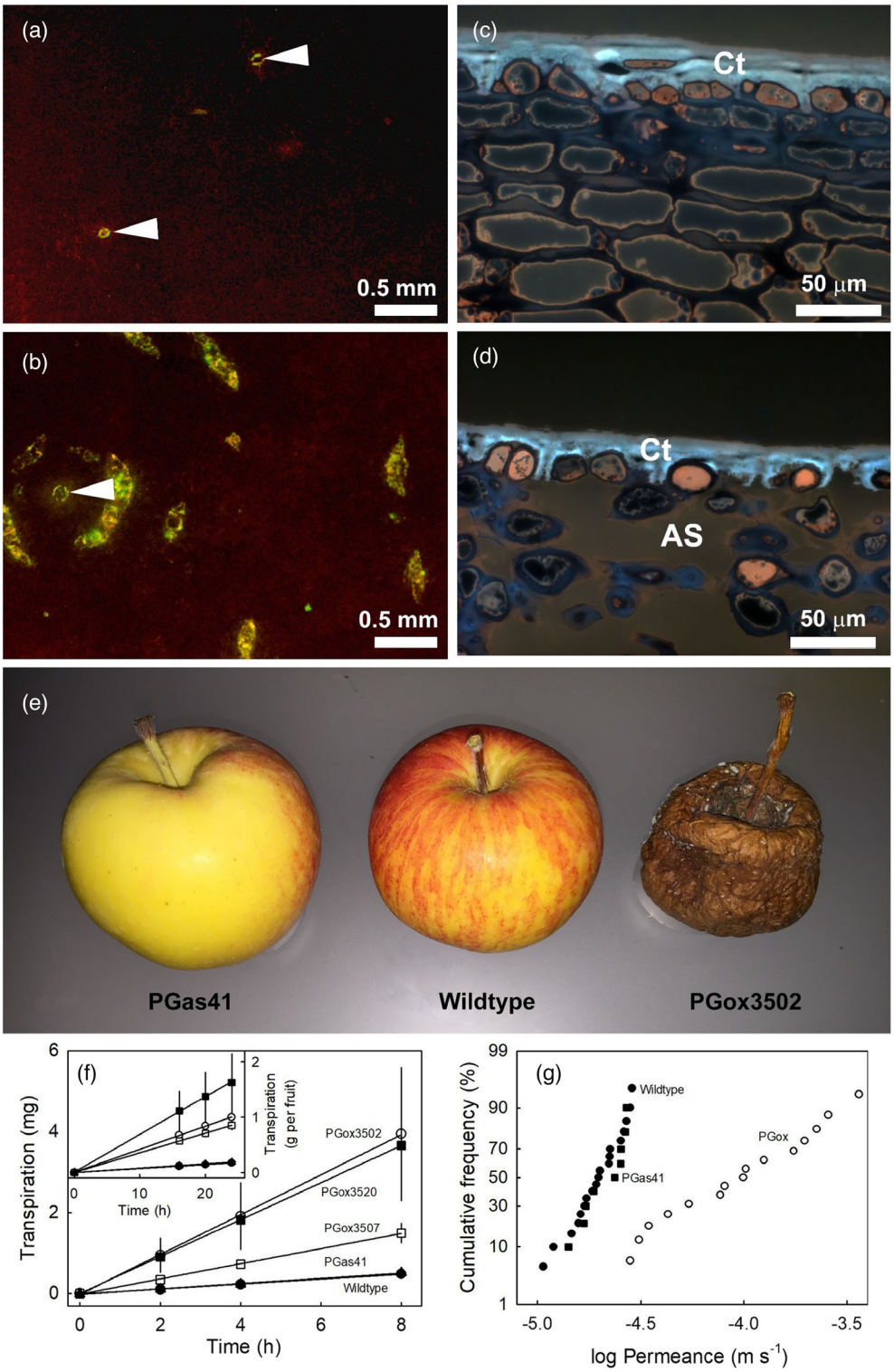

Figure 4. Apple fruit cuticular integrity and fruit water loss.
(a, b) Fluorescence micrographs of apple fruit surfaces after immersion in aqueous acridine orange solution.
(a) Wildtype (WT).
(b) PGox3502. Fluorescing areas characterise sites where dye penetration into the tissue bypassed the cuticle barrier and represent cracks that occurred consistently around lenticels in the PGox apple. White arrowheads indicate lenticels.
(c, d) Representative transverse sections showing cuticles are similar in thickness and morphological structure, as shown by autofluorescence with UV excitation.
(c) Wildtype.
(d) PGox3502.
(e) Appearance of fruit from a PG antisense line (PGas41), WT and PGox3502 after 4 weeks post-harvest at 21°C.
(f) Time course of transpiration of excised skin segments and of whole fruit (inset) of WT, PGox lines (3502, 3507 and 3520) and PGas41. Fruit were assayed at approximately 70 days after pollination. Data are means ± SE. n.b. PGas41 and WT data points overlap.
(g) Cumulative frequency distribution plot of log-transformed permeance of excised skin segments. The three PGox lines (3502, 3507 and 3520) were combined in panel g.

Table 1 Permeance (P) of skin segments excised from the equatorial plane of wildtype, polygalacturonase (PG) antisense (PGas41) and three PGox (3502, 3520, 3507) lines of apple fruit.

	P ($\times 10^{-5}$ m•sec^{-1})					
				Range		
Genotype	*n*	Mean ± SE	Median	Min.	Max.	cv (%)
Wildtype	20	2.1 ± 0.1 a	2.0	1.1	3.8	30.8
PGas41	10	2.2 ± 0.2 a	2.4	1.4	2.9	23.5
PGox3502	8	5.6 ± 0.9 b	4.9	2.8	10.0	47.6
PGox3520	6	20.8 ± 3.9 b	20.0	10.2	36.1	45.8
PGox3507	2	39.3 ± 16.0 b	39.3	19.7	58.8	70.4
PGox (all)	16	15.5 ± 3.7	10.1	2.8	58.8	96.4

Statistical analysis followed by Tukey's range test. Means ± SE with the same letter were not different at the $P < 0.05$ level. cv = % coefficient of variation.

transcription factor (*MYB10*) (Espley et al., 2007) was at higher abundance in the peel of WT fruit and increased as the fruit matured (Table S3). Consistent with this higher expression, the anthocyanin biosynthetic genes *4CL*, *CHS*, *LDOX* and *UGT78D2* were also significantly upregulated (Table S3).

To complement the above univariate analysis, multivariate analysis was carried out using partial least squares discriminant analysis (PLS-DA). Since high variability was observed in the 80 DAP samples, these samples were removed from further analysis. A four-class supervised PLS-DA was carried out using the 60 and 100 DAP samples to identify the transcripts that best discriminated the groups (Figure 7b). In this analysis, samples were distributed along component 1 (76.8% of the variance) following chronological age, with the PGox3502 samples appearing more advanced in biological age. Component 2 (15.4% of the variance) separated the samples by genotype. The genes with the top two variable importance on projection (VIP) scores were the transgene (*MdPG1*) and *ACO1*. The 200 genes that had the highest VIP scores were selected and converted to TairIDs, and used as input into the DAVID Gene Functional Classification Tool (Huang et al., 2009). Of these, 122 genes were successfully converted in DAVID IDs. Gene Ontology (GO) terms enrichment analysis highlighted the most relevant GO terms associated with this list (Figure 7c). The most highly enriched biological theme was 'salicylic acid catabolic process' (98.8-fold enrichment), with other stress-related themes ('hydrogen peroxide catabolic process', 'fatty acid metabolic process' and 'response to oxidative stress') also showing strong enrichment. The theme 'response to abscisic acid' is consistent with the water-stressed nature of the fruit. Several cell wall-related themes were also enriched ('plant-type cell wall biogenesis', 'cell wall biogenesis' and 'cell wall organization'), indicating widespread effects on cell wall metabolism.

DISCUSSION

Constitutive overexpression of *MdPG1* in apple plants had pleiotropic effects, with changes to plant appearance, growth, stress resistance and physiology. Multiple effects on the fruit were observed, including accelerated development and softening, accelerated seed development and changes to the fruit outer cell layers with related effects on water loss. The most striking visual phenotype in the fruit, which occurred from as early as 60 DAP, was the development of a white skin that most likely resulted from additional light scattering due to separation of the epidermal layers from the hypodermis. By 120 DAP, fruit from many lines showed severe cracking, shrivelling and pathogen infections, meaning they did not survive to undergo the normal ripening process (which begins at this time in WT fruit). In comparison with WT fruit at the same chronological age based on DAP, cell walls from the peels of PGox lines appeared thinner with reduced cell wall content on a tissue FW basis, showed a higher yield of WS pectin, and a lower galactose content (Figure 5). Cell walls from the cortex exhibited similar trends in many cases, but to a lesser extent.

Fruit firmness is a composite of middle lamella strength, cell wall strength and cell turgor, and overexpression of *MdPG1* probably affected all three of these parameters. The most prominent phenotypic effect of overexpression of *MdPG1* on the fruit was alterations to

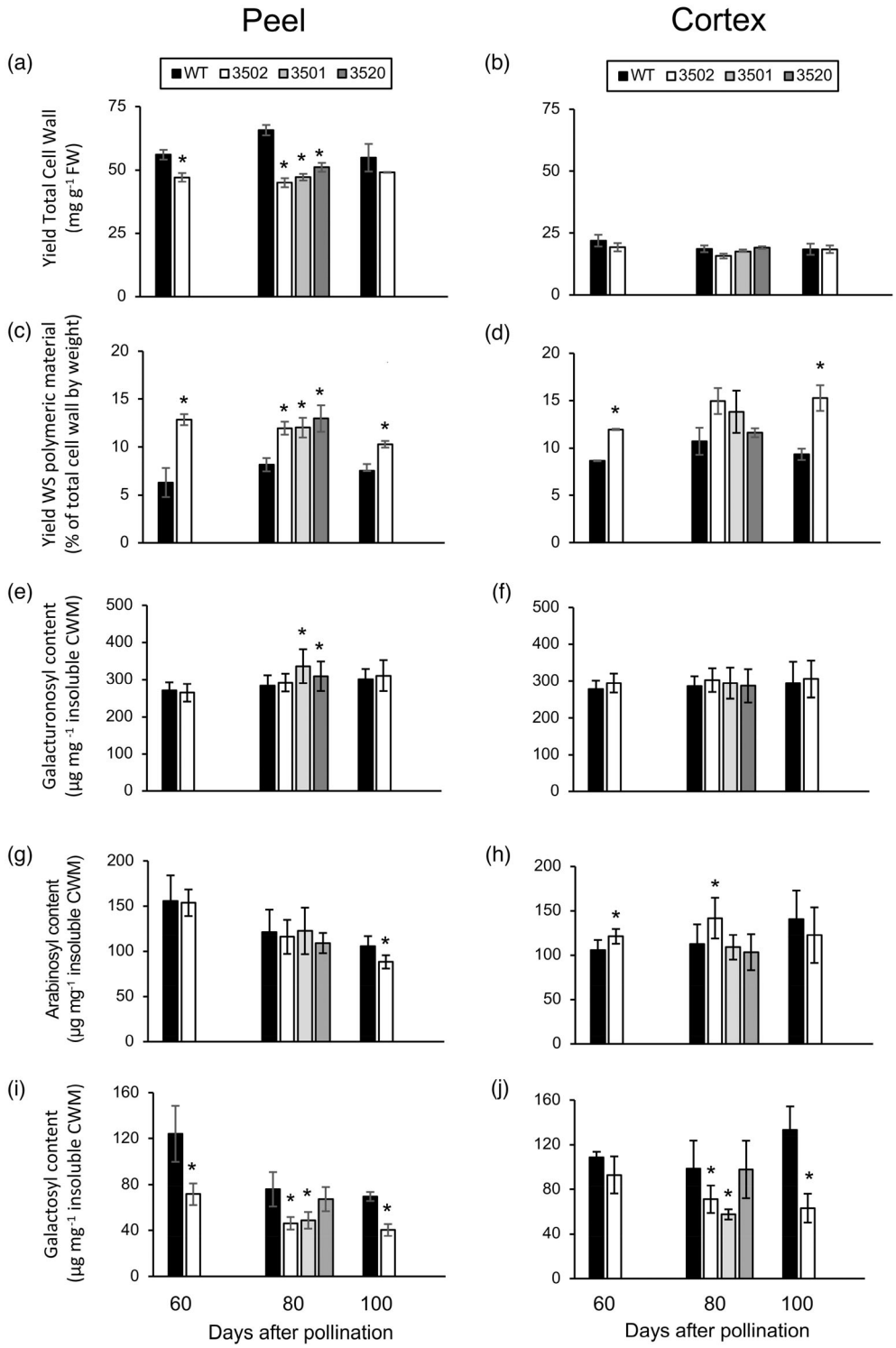

Figure 5. Cell wall characteristics of apple fruit peel and cortex in PGox lines relative to wildtype (WT).
(a, b) Yield of total cell walls on a fresh weight (FW) basis.
(c, d) Water-soluble cell wall material (CWM) as a percentage of total CWM.
(e, f) Galacturonosyl content of insoluble CWM.
(g, h) Arabinosyl content of insoluble CWM.
(i, j) Galactosyl content of insoluble CWM. Asterisks denote samples statistically different from the WT ($P = 0.05$) at the same days after pollination using Student's *t*-test.

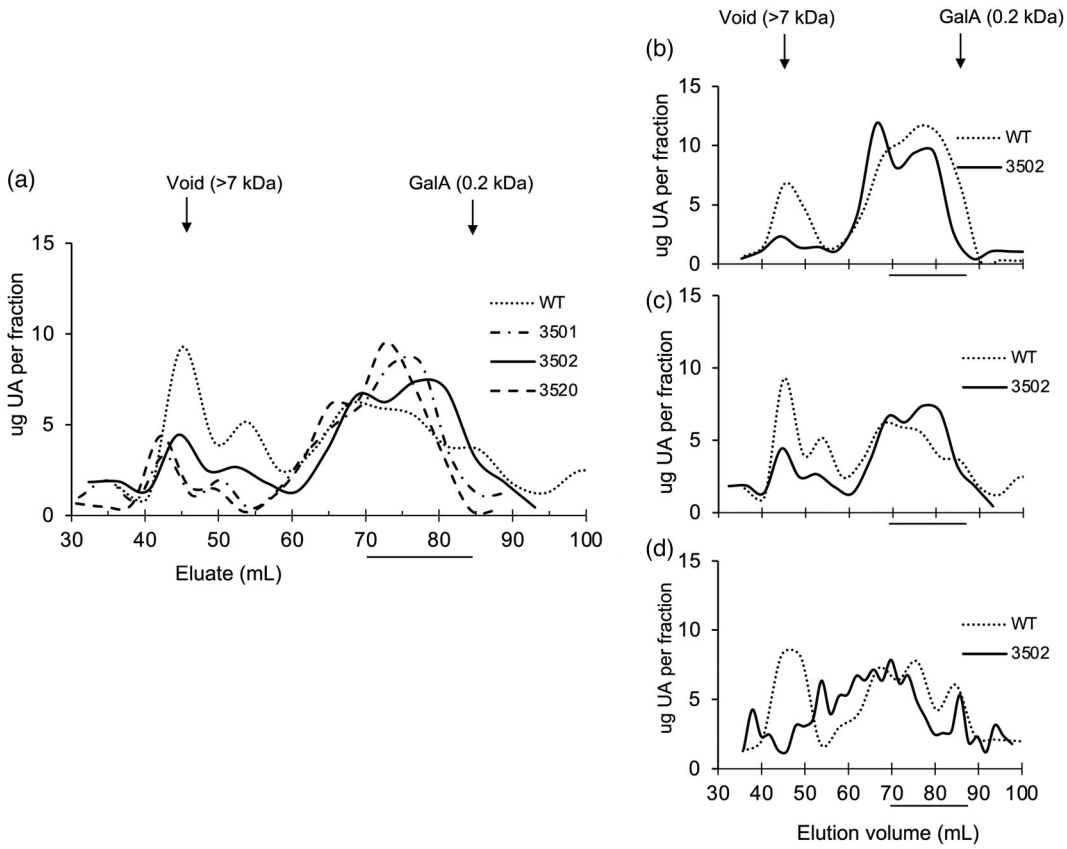

Figure 6. Oligogalacturonides (OGs) from wildtype (WT) and PGox apple fruit.
(a) OGs were extracted from cortex tissue of WT and PGox lines 3502, 3501, 3520. Comparison of OG abundance in WT and three transgenic lines at 80 days after pollination (DAP).
(b–d) Comparison of OG abundance in WT and line 3502 at 60, 80 and 100 DAP, respectively. OG-enriched extracts were eluted over a HWS40F column and elution profiles monitored by uronic acid content of each 1-ml eluate fraction. The bar below each graph indicates the elution position of biologically active OGs with a degree of polymerisation of 4–6.

the structure of the epidermis and outer cell layers. The outer cell layers became disorganised with substantial cell separation, accompanied by the appearance of large air spaces below the epidermis (Figure 3d–f), and a substantial increase in WS pectin (Figure 5c), presumably due to degradation of the HG-rich middle lamellae that also causes reduced intercellular adhesion (Wang et al., 2018). This observation is consistent with the converse effect of silencing *MdPG1*, where the hypodermal layers below the epidermis became more compact and water loss was reduced, leading to firmer fruit (Atkinson et al., 2012). Similarly, silencing of *SlPL* in tomato resulted in more compact cells and reduced water loss (Yang et al., 2017). There is also evidence that the primary cell wall structure was affected, since galactosyl content was reduced in the PGox line (Figure 5i), and the appearance of linear arabinan in deeper cell layers was accelerated during development (Figure 3k,l). The galactosyl content of fruit cell walls has been correlated with hardness/stiffness (Ng et al., 2015; Yang et al., 2022), and the appearance of linear arabinan is believed to be due to the trimming of existing branched arabinan, and normally spreads from epidermal cells to cortical cells late in fruit development (Collins et al., 2019). The early appearance of the linear arabinan LM13 epitope in hypodermal and cortical cells provides additional evidence for advanced fruit maturity in the PGox lines.

A dramatic result of the altered skin structure was greatly increased water permeance and subsequent postharvest fruit water loss. Increased skin cracking can be a consequence of altered cell wall structure, as shown in tomato where the cell wall structure was affected by silencing of the β-galactosidase gene *TBG6*, silencing of *SlEXP1/SlPG2a*, or by overexpression of the grape PL *VvPL1* (Jiang et al., 2019; Moctezuma et al., 2003; Yu et al., 2023). The higher permeance of apple fruit in the PGox lines was also related to microcracking of the cuticle. Fluorescence microscopy revealed penetration of the tracer acridine orange through microcracks in the cuticle of the PGox lines, but not in the WT (Figure 4). These microcracks impair the barrier function of the cuticle and allow the

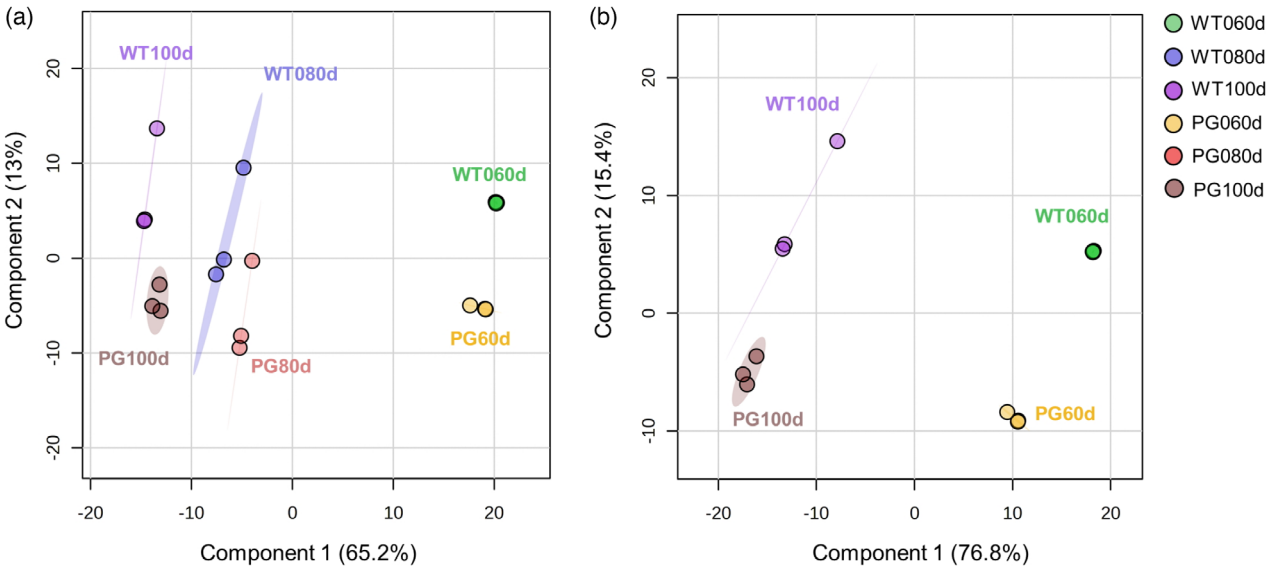

(c)

Term	RT	Genes	Count	%	P-Value	Fold Enrichment	Benjamini
salicylic acid catabolic process	RT		2	1.6	2.0E-2	98.8	6.4E-1
rhythmic process	RT		3	2.5	9.3E-3	20.4	3.9E-1
negative regulation of transcription from RNA polymerase II promoter	RT		3	2.5	2.3E-2	12.6	6.4E-1
shoot system morphogenesis	RT		4	3.3	7.4E-3	10.0	3.6E-1
plant-type cell wall biogenesis	RT		5	4.1	4.2E-3	7.6	3.1E-1
cell wall biogenesis	RT		6	4.9	1.5E-3	7.2	1.6E-1
alpha-amino acid metabolic process	RT		4	3.3	2.4E-2	6.4	6.4E-1
circadian rhythm	RT		4	3.3	2.4E-2	6.4	6.4E-1
hydrogen peroxide catabolic process	RT		3	2.5	8.4E-2	6.2	1.0E0
cell wall organization	RT		9	7.4	1.5E-4	5.9	4.3E-2
fatty acid metabolic process	RT		3	2.5	9.6E-2	5.7	1.0E0
meiotic cell cycle process	RT		4	3.3	3.9E-2	5.3	8.7E-1
cellular response to lipid	RT		5	4.1	9.1E-2	2.9	1.0E0
tissue development	RT		11	9.0	6.1E-3	2.8	3.6E-1
macromolecule biosynthetic process	RT		14	11.5	1.6E-3	2.8	1.6E-1
response to oxidative stress	RT		8	6.6	2.8E-2	2.7	7.0E-1
response to lipid	RT		8	6.6	8.0E-2	2.1	1.0E0
response to abscisic acid	RT		10	8.2	7.8E-2	1.9	1.0E0

Figure 7. Transcriptomic comparison of wildtype (WT) and PGox3502 apple.
Replicated RNA-Seq samples were prepared from fruit peel of WT and PGox3502 (PG).
(a) PCA scores plot at 60, 80 and 100 days after pollination (DAP).
(b) PLS-DA scores plot at 60 and 100 DAP. Both the PCA and PLS-DA were generated using the top 5000 differentially expressed genes (DEGs).
(c) Enriched biological themes in highly DEGs between PGox3502 and WT fruit peel. Enriched Gene Ontology terms were identified using the DAVID Gene Functional Classification Tool (Huang et al., 2009).

passage of water vapour across the skin (Maguire et al., 1999). In apple, epidermal and hypodermal cell layers represent the structural backbone of the fruit skin (Khanal & Knoche, 2014), and the cuticle is stretched as the fruit skin is strained by growth stresses. The reduced cell-to-cell adhesion caused by overexpression of *MdPG1*, resulting in the formation of large intercellular spaces, decreases the fracture force of the fruit skin, producing microcracking of the cuticle and ultimately even cracking of the whole fruit (Knoche & Lang, 2017). That microcracks occurred around lenticels is not surprising. Lenticels represent sites of stress concentration that focus tangential growth stress in this particular region (Knoche & Lang, 2017). Ultimately, the greatly increased water loss of PGox fruit would reduce cell turgor and contribute to enhanced post-harvest fruit softening.

An unexpected result of the overexpression of MdPG1 was the advancement of fruit development (Figure 2). This early-maturation phenotype may be related to the production of physiologically active OGs from partial hydrolysis of HG by MdPG1, and at 80 DAP, all PGox lines produced more OGs of 4–6 DP than the WT (Figure 6a). This may be

Table 2 Differentially expressed genes related to cell wall metabolism, ethylene biosynthesis/action and heat response in apple fruit peel of PGox3502 relative to wildtype. GDDH gene model and description from the Genome Database for Rosaceae (Jung et al., 2019).

GDDH Gene ID	60 DAP logFC	100 DAP logFC	Description
Cell wall			
MD10G1179100	13.495223	12.850444	MdPG1 (transgene)
MD15G1221000	2.853321	2.093149	β-Galactosidase 7
MD02G1079200	2.316354	n.s.	β-Galactosidase 12
MD15G1206800	n.s.	2.262637	β-Galactosidase 12
MD01G1135600	2.139594	n.s.	Expansin A4
MD09G1152600	n.s.	3.778415	Xyloglucan endotransglucosylase/hydrolase 16
MD16G1106400	−2.10744	n.s.	Pectate lyase
MD01G1068900	n.s.	−2.00557	Pectin lyase-like superfamily protein
MD06G1161400	n.s.	−2.34009	Pectin lyase-like superfamily protein
MD08G1195600	n.s.	2.357203	Pectin methylesterase inhibitor family
MD13G1149800	−2.51791	n.s.	Pectin methylesterase inhibitor family
MD07G1255400	n.s.	−4.00443	Pectin methylesterase inhibitor family
MD17G1099500	2.565262	n.s.	Cellulose synthase-like B3
MD17G1099600	2.597678	n.s.	Cellulose synthase-like B4
MD17G1042500	n.s.	2.426155	Galacturonosyltransferase-like 10
Ethylene			
MD12G1201100	2.007531	2.522308	S-Adenosylmethionine synthase 1
MD14G1111500	2.045756	3.065303	ACC synthase 6
MD06G1090600	2.45224	n.s.	ACC synthase 6
MD15G1203500	n.s.	2.304924	ACC synthase 7
MD17G1106300	2.917106	n.s.	ACC oxidase
MD05G1030800	2.250868	n.s.	Ethylene response factor 110
Heat response			
MD02G1139900	2.137417	n.s.	Dehydrin family protein
MD15G1253900	n.s.	−2.22319	Dehydrin zero 1
MD01G1144300	2.551809	n.s.	Heat shock protein 18.2
MD01G1144400	2.438214	n.s.	Heat shock protein 18.2
MD07G1210400	3.482866	n.s.	Heat shock protein 18.2
MD07G1210700	3.208756	n.s.	Heat shock protein 18.2
MD08G1068000	4.282116	n.s.	17.6 kDa class II heat shock protein
MD08G1068200	4.113046	n.s.	17.6 kDa class II heat shock protein
MD08G1068300	4.123406	n.s.	17.6 kDa class II heat shock protein
MD08G1068400	4.333719	n.s.	17.6 kDa class II heat shock protein
MD13G1108500	4.761318	n.s.	Heat shock protein 21
MD17G1209800	2.784448	n.s.	HSP20-like chaperones superfamily protein

Relative mRNA abundance is given at 60 and 100 days after pollination (DAP). Negative logFC values indicate gene downregulation and positive values upregulation. Genes shown had expression abs(logFC) ≥2 and > 300 counts in at least one sample. n.s. = not significant at this stringency. The full list of genes with expression abs(logFC) ≥2 and *P*-value <0.05 is shown in Table S3.

the *in vivo* signal leading to the increased ethylene production observed in the PGox fruit starting at approximately 80 DAP. Such OGs are known elicitors of plant defence, are involved in local wound responses and can regulate developmental processes as antagonists of auxin (Ferrari et al., 2013). OGs with a DP of 10–15 have been associated with plant defence responses against microbial attack, whilst smaller OGs (4–6 DP) stimulate ripening in tomato fruit through the induction of ethylene (Ma et al., 2016; Simpson et al., 1998). However, the observation that populations of short OGs produced from apple pectin by the action of fungal PG unexpectedly delayed fruit softening in tomato (Yang et al., 2022) suggests that the features determining the specificity of active OGs (DP plus potentially methyl-esterification or acetylation pattern) require further investigation.

Overexpression of *MdPG1* accelerated fruit maturity, as evidenced by early changes to seed colour, starch/sugar metabolism, expression of genes related to ethylene biosynthesis, softening and appearance of the LM13 cell wall epitope in hypodermal and cortical cells. This advancement in fruit maturity may be related to the changes in vegetative growth observed in the PGox lines (Figure S1a). The weak growth habit of the PGox lines and sensitivity to dehydration likely places stress on fruit development. This can be seen in the reduced size of PGox fruit compared with WT, even though fruit load on WT and PGox lines was managed to be similar. The advancement of maturity

does not appear to be regulated through two transcription factors known to advance fruit maturity in apple, *NAC18.1* (MD03G1222600) (Migicovsky et al., 2021) and *MYB10* (MD09G1278600) (Espley et al., 2019). The expression of *NAC18.1* was similar in PGox and WT, whilst expression of *MYB10* was upregulated in WT compared with PGox (Table S3).

When mechanically wounded or subjected to infection, plants under field conditions will accelerate fruit development and ripening to ensure that seed is viable for dispersal. Transcriptomic analysis of the peel tissue from PGox and WT fruit suggested that the advancement in maturity may be a feature of the stresses PGox fruit are under during development. These stresses include greatly increased water permeance and reduced cell wall strength and cell turgor. Transcriptomic comparison of PGox and WT fruit revealed a relatively small number of DEGs (approximately 1000) in peel at 60 and 100 DAP. However, pathways involved in abiotic stress responses and phenylpropanoid metabolism were differentially regulated in outer cell layers (Figure 7c). Genes with a differential expression of >4-fold at 60 and 100 DAP showed altered regulation of a number of genes related to cell wall metabolism, including pectin modification and cell wall synthesis (Table 2). At 60 DAP, two β-galactosidases were upregulated, which may possibly be involved in the reduced cell wall galactosyl content. Ethylene production in the fruit was also advanced, to a chronological age well before this occurs in the WT (Figure 2g), along with early upregulation of three ACS genes, an ACC oxidase and an ethylene response factor (Table 2). These findings are consistent with the accelerated development of the PGox fruit and evidence for earlier onset of the ripening process. The stressed condition of the PGox fruit was further illustrated by the strong upregulation of a dehydrin and a suite of heat shock and chaperonin proteins (Table 2), and enriched themes related to a range of oxidation, dehydration and stress responses (Figure 7c). Several cell wall-related themes were also strongly enriched.

Other studies have also found that transgenic manipulation of one cell wall-related gene altered the expression of other cell wall-related genes. In tomato, silencing of *SlPL* reduced expression of genes encoding an EXP, a PG, an XTH and a cellulose synthase (Yang et al., 2017). In strawberry, silencing of both *FaPG1* and *FaPG2* also downregulated a range of genes encoding proteins involved in cell wall modification (Paniagua et al., 2020). Also in strawberry, transient overexpression in fruit of two different PME genes upregulated a PL and a PG gene (Xue et al., 2020). Consistent with our findings, other studies have also found that manipulation of a single cell wall-related gene can affect fruit ripening and softening. In tomato, constitutive overexpression of persimmon *DkXTH8* led to advanced ethylene production, accelerated fruit colour change and increased softening (Han et al., 2016), as did overexpression of the persimmon β-galactosidase *DkGAL1* (Ban et al., 2018). Changes to cell shape and packing were also observed (Han et al., 2016), although there were no deleterious effects on fruit condition (Ban et al., 2018). In strawberry, transient overexpression of *FvXTH9* or *FvXTH6* accelerated ripening and softening (Witasari et al., 2019), and in peach transient silencing of the β-galactosidase genes *PpBGAL10* or *PpBGAL16* slowed ripening and softening by reducing ethylene production and expression of the ethylene-regulated *PpPG* gene (Liu et al., 2018). Taken together, these studies show that manipulation of the expression of a single cell wall-modifying gene can have wide-ranging effects on fruit ripening and softening. The mechanisms by which cell wall structure and function are monitored by the cell (Du et al., 2022; Wolf, 2022), and feed back to affect gene expression and fruit development (Jia et al., 2023), is an exciting area for future research.

EXPERIMENTAL PROCEDURES

Generation and growth of transgenic plants

The fruit-specific apple PG gene *MdPG1* (Atkinson, 1994) was ligated into pART7 to produce a *35S:PG1:nos* cassette and then into the pART27 binary vector, as described in Atkinson et al. (2002). pART27-PG1 was introduced into *Agrobacterium tumefaciens* strain LBA4404 by electroporation and used to generate 20 independent PGox transgenic *Malus domestica* (Borkh.) 'Royal Gala' apple plants (Yao et al., 1995). Transgenic plants were micro-grafted onto 'M9' rootstocks and grown in a containment glasshouse alongside untransformed grafted 'Royal Gala' WT controls. Replicated transgenic plants and controls were obtained by macro-grafting onto 'M9' rootstocks. All plants were grown under the same natural daylight and temperature conditions in 8.5-L planter pots. However, PGox lines received supplemental watering and did not receive the winter chilling (8 weeks at 7°C) given to the WT to promote and synchronise flowering. Flowers were individually labelled and hand-pollinated each spring using 'Granny Smith' pollen. PGox trees typically carried <10 fruit per plant. Fruit on WT trees were thinned to approximately 20 fruits per tree. Generation of the *MdPG1* antisense line PGas41 is described by Atkinson et al. (2012).

Physiological assessments of fruit

Fruit were harvested at defined chronological ages based on DAP. Harvests at 60, 80 and 100 DAP were used for most analyses. Cortical firmness was measured by puncture tests using a Stable Micro Systems TA.XT*Plus* Texture Analyser (Godalming, UK) using an 7.9-mm Effegi penetrometer probe as described by Johnston et al. (2009). Soluble solids content was measured using a digital refractometer (Atago, Model PAL-1, Japan). Skin colour measurements were obtained using a chromameter (Konica Minolta, model CR-300, Tokyo, Japan). Internal ethylene concentration was determined by extracting a 1-mL core cavity gas sample and injecting it into a gas chromatograph (5890 series II, Hewlett Packard, Wilmington, DE, USA) as described by Johnston et al. (2009). Assessments were carried out on five fruits per genotype at each time point. Starch measurements were carried out according to

the method of Smith et al. (1992), using three biological replicates per time point measured with two technical replicates.

Chlorophyll quantification was carried out after Ampomah-Dwamena et al. (2015) and Bhargava et al. (2023). In brief, approximately 300 mg of frozen powdered peel tissue was extracted in acetone containing 0.1% butylated hydroxytoluene. The extracts were shaken with di-ethyl ether, the organic phase recovered, dried and taken up in ethanol containing 0.1% butylated hydroxytoluene. Quantification was carried out using a Waters Acquity UPLC system (Milford, MA, USA) equipped with a photodiode array detector. An aliquot of 10 μl was injected onto an Acquity UPLC BEH C18 column (2.1 × 50 mm, 1.8 μm particle size, Waters, Milford, MA, USA) at 40°C and a flow rate of 0.5 $ml \bullet min^{-1}$ and separated using a gradient of 0.1% formic acid in water and 0.1% formic acid in acetonitrile. Chlorophylls and derivatives were detected at 420, 430 and 450 nm according to absorption maxima, quantified using a six-point calibration curve and presented as total chlorophyll.

Anthocyanins were extracted from 10 to 15 mg freeze-dried peel tissue using methanol containing 0.1% HCl. After centrifugation, the absorption of extracts was determined photometrically at 530 and 657 nm. Quantification of anthocyanins was carried out using the following equation: Anthocyanins = [OD530–0.25 x OD657] x TV / dry weight (DW) of tissue × 1000 (OD = optical density; TV = total volume of the extract in mL; DW of tissue in mg). Chlorophyll and anthocyanin determinations were carried out using three biological replicates per time point and genotype.

Light microscopy, immunolabelling and cryo-SEM

Light microscopy and immunolabelling were carried out on WT and PGox fruit at 60, 80 and 100 DAP. Skin and outer cortex tissue for optical microscopy was fixed in 2% (v/v) paraformaldehyde and 2.5% (v/v) glutaraldehyde in 0.1 M phosphate buffer (pH 7.2) at ambient temperature and then stored at 4°C. Subsequently, samples were dehydrated in an ethanol series, embedded in LR White resin (Sutherland et al., 2009) and sections cut using a Leica UCT ultramicrotome (Leica Microscopy Systems Ltd, Heerbrugg, Switzerland). Sections 1000 nm thick were used for structural observation and were stained with a 0.05% (w/v) solution of toluidine blue in benzoate buffer (pH 4.4). Resin sections 200 nm thick were used for immunolabelling of pectic material (Sutherland et al., 2009). Primary antibodies used for immunolabelling were JIM5 and LM20, which detect low and high methyl-esterified HG, respectively, LM6 to short regions of (1 → 5)-α-L-arabinan backbone and branches, and LM13 to linearised (1 → 5)-α-L-arabinan, the latter being selected on the basis of work reported by Collins et al. (2019). Secondary antibody reactions and visualisation were carried out as described by Collins et al. (2019). All antibodies were sourced from PlantProbes (Leeds, UK).

CryoSEM was carried out on WT and PGox fruit at 120 DAP. Segments of tissue including skin and underlying cortex were mounted vertically in sample holders and frozen, processed and imaged as described by Woolf et al. (2013) using a Polaron PP2000 Cryo Transfer System (Quorum Technologies, Ringmer, UK) attached to a FEI Quanta 250 Scanning Electron Microscope (FEI, Hillsboro, OR, USA).

The occurrence of microscopic cracks in the cuticle was examined by submerging an equatorial portion of the fruit in a 0.1% (w/v) aqueous acridine orange solution for 10 min (Peschel & Knoche, 2005). Fruit were carefully rinsed with deionised water and blotted with soft tissue paper. The stained region of the fruit was then viewed using a fluorescence microscope (MZ10F; Leica Microsystems, Wetzlar, Germany).

Transpiration assays

Transpiration was quantified on a whole-fruit and an excised skin segment basis using fruit harvested at approximately 70 DAP. Fruit free of visual defects were selected, but numbers for some lines were restricted by availability (recorded in Table 1). The stem was removed, and the cavity and calyx sealed with a non-phytotoxic silicone rubber (Dow Corning 3140 RTV Coating; Dow Corning, Midland, Michigan, USA), thereby restricting water transport to the fruit surface. Fruit were incubated in polyethylene boxes above dry silica gel. Transpiration was quantified gravimetrically. Rates of transpiration (F; $g \bullet h^{-1}$) were obtained from a linear regression line fitted through a plot of cumulative weight loss versus time.

Transpiration through the excised skin segments was determined as described by Knoche et al. (2000). Briefly, the segments were prepared by cutting tangentially underneath the skin. The cap of a sphere so obtained comprised the cuticle, the epidermis and hypodermis and several layers of cortical cells. The segments were mounted on stainless steel diffusion cells using a high vacuum grease. Diffusion cells were filled with deionised water. The lid was tape-sealed to the bottom. The port in the bottom was also tape-sealed so that transpiration was restricted to the surface of the segment exposed in the orifice of the diffusion cell. Diffusion cells were then incubated in a PE box above dry silica and weighed at selected time intervals. Rates of transpiration (F; $g \bullet h^{-1}$) were calculated as described above. Thereafter, the permeance (P) was calculated from F, the area of the segment exposed in the orifice of the diffusion cell (A) and the difference in water vapour concentration (ΔC) between the inside of the diffusion cell and that above the dry silica gel according to the equation:

$$P = \frac{F}{\Delta C \times A}$$

The water vapour concentration above dry silica is assumed to be zero (Geyer & Schönherr, 1988), whilst that in the diffusion cell is in equilibrium with liquid water, that is at saturation.

Cell wall preparation, extraction and analyses

Cell wall material and extracts were prepared from fruit at 60, 80 and 100 DAP from a single season, using two biological replicates per line per time, each consisting of four fruit. Biological replicates were analysed using three technical replicates. Peel (thinly pared shavings from the fruit surface, including some outer cortex) and cortex (combination of outer and inner) were snap-frozen in liquid N_2 and ground to a fine powder. Cell walls were prepared and extracted as described by Fullerton et al. (2020). In brief, buffer-saturated phenol (Invitrogen, Carlsbad, CA, USA) was used to inactivate tissue, and the pellet was washed twice with water. Phenol- and water supernatants were combined and dialysed against water to give the WS polymeric extract. To remove starch, the pellet was extracted twice with 90% (v/v) dimethyl sulfoxide over a total of 5 days. The remaining pellet was dialysed and freeze-dried to give the insoluble CWM. The sum of the yields of WS polymeric material and insoluble CWM is defined as 'total cell wall material'. Aliquots (100 mg) of insoluble CWM were extracted with 50 mM CDTA (trans-1,2-diaminocyclohexane-N,N,N-′N′-tetra-acetic acid), followed by 50 mM Na_2CO_3. CDTA-soluble supernatants were dialysed (3 kDa molecular weight cut-off, Sigma-Aldrich, St Louis, MO, USA) against ammonium acetate buffer (pH 5.2) followed by H_2O and freeze-dried to give the CDTA-soluble extract. Na_2CO_3-soluble supernatants were dialysed against water and freeze-dried to give the Na_2CO_3-soluble extract.

Neutral sugar content was determined by gas chromatography after hydrolysis in trifluoroacetic acid, followed by the conversion of monosaccharides to alditol acetates (Albersheim et al., 1967) as described by Prakash et al. (2017). UA contents were determined as described by Ahmed and Labavitch (1977) and Blumenkrantz and Asboe-Hansen (1973) with GalA as a standard. The degree of pectin methyl-esterification (DE) was determined by gas chromatographic quantification of methanol after saponification of pectin as described by Ng et al. (2013) and calculated as a molar ratio of methanol to UA.

For size exclusion chromatography, water-, CDTA- and Na_2CO_3-soluble fractions were hydrated in water (1 mg•mL^{-1}) and eluted through a column of Superose 6 (1 × 30 cm; eluent 0.05 M ammonium acetate buffer pH 5.0; flow rate 0.5 ml•min^{-1}). Fractions (0.25 ml) were collected and UA content determined according to the method of Blumenkrantz and Asboe-Hansen (1973).

Purification of pectic oligosaccharides

Frozen (−80°C) cortex tissue (50 g) of WT and PGox fruit at 60, 80 and 100 DAP was finely ground and extracted in >85% (v/v) ethanol using a Polytron. The suspension was centrifuged, the pellet was washed three times with 85% ethanol, and all supernatants discarded. Oligosaccharides were solubilised by extracting the pellet with 50% ethanol followed by water, and supernatants recovered by centrifugation. Supernatants were evaporated to dryness using a rotary evaporator and taken up in water. Pectic oligosaccharides were enriched by ultrafiltration using a 100 kDa membrane to remove soluble polysaccharides followed by a 10 kDa membrane (Amicon). The flow-through of the 10 kDa membrane (potentially containing pectic oligosaccharides) was subjected to anion exchange chromatography on QAE Sepharose equilibrated in water (Pharmacia; H^+ form). The bound fraction was eluted using 10% formic acid, evaporated to dryness to remove formic acid, taken up in water and subjected to gel filtration chromatography on HWS40F (Toyopearl) (column 1.2 × 120 cm; flow rate 6 ml•h^{-1}, fraction size 20 min, eluent 1% pyridine and 1% acetic acid in water). The UA content of each fraction was determined as described above.

Polyacrylamide gel electrophoresis and Western blot analysis

Total proteins were extracted from leaves by boiling 100 mg of finely ground tissue in 0.5 ml of extraction buffer (0.1 M Bis-Tris, 2 M glycerol, 0.3 M sodium dodecyl sulphate, 0.2 M dithiothreitol, 0.01% (w/v) Coomassie brilliant blue G) for 10 min. After centrifugation (10 min, 11 000 ***g***), the supernatants (10 µl) were loaded onto 10% polyacrylamide gels and proteins separated by electrophoresis.

Total proteins in fruit peel or cortex were extracted in buffer containing 7 M urea, 2 M thiourea, 40 mM Tris–HCl, 75 mM dithiothreitol and 4% CHAPS (1 ml buffer per 100 µg tissue). Protein content was determined from the supernatant after centrifugation using Bio-Rad protein reagent with bovine serum albumin as a standard. Samples were denatured by boiling in SDS buffer containing Coomassie Brilliant Blue G for 1 min, then equal amounts of protein (1 µg per lane) were loaded onto polyacrylamide gels. Polyacrylamide gel electrophoresis, protein gel blotting and immunostaining were carried out as described by Fullerton et al. (2020) using polyclonal antibodies raised against MdPG1 (Atkinson et al., 2012). Western blots were scanned with a high-resolution scanner and images adjusted for brightness.

Transcriptomic and bioinformatic analysis

For both the PGox transgenic line and the WT control, total RNA from fruit peel was extracted from three biological replicates (each consisting of tissue from four fruits) at each time point as described by Chang et al. (1993). RNA quality and quantity were measured using an RNA Fragment Analyser (Agilent, Santa Clara, CA, USA). RNA-Seq libraries were prepared and sequenced at the Australian Genome Research Facility (AGRF), Melbourne, on an Illumina HiSeq2000 platform in paired-end mode with read length of 150 bp. Raw sequencing data were downloaded from AGRF, and data integrity was confirmed with md5sum values. The samples were processed consistently in parallel. Data quality was checked using FastQC-0.11.2 (https://www.bioinformatics.babraham.ac.uk/projects/fastqc/). Based on the quality report, raw reads were cleaned with fastp-v0.20.0 (Chen et al., 2018). The cleaned reads were mapped to the GDDH genome (Daccord et al., 2017) with hisat2/2.1.0 (Kim et al., 2019), alignments were sorted and indexed with samtools/1.10 (Li et al., 2009), and read counts were extracted with featureCounts in the subread package. Differential expression analysis was performed between the transgenic line and the WT control samples with DESeq2_1.28.0 (Anders, 2010). Enriched GO terms were identified using the DAVID Gene Functional Classification Tool (Huang et al., 2009). The 200 genes with the highest VIP scores from the PLS-DA were first converted to TAIR IDs and used as input into DAVID, where they were converted to Entrez IDs. Transcriptomic data are available upon request.

Statistical analyses

Unless stated otherwise, Microsoft® Excel 2013 was used to perform two-tailed t-tests to calculate the significance of sample means ($P < 0.05$) between genotypes. Principal component analysis (PCA) and partial least square discriminant analysis (PLS-DA) were performed using $\log_{10}$-transformed data with the MetaboAnalyst 5.0 online platform (www.metaboanalyst.ca). PCA and PLS-DA were generated using the top 5000 most DEGs. MetaboAnalyst filtered genes based on the interquartile range (removal of genes with expression that was near constant throughout the given experimental conditions). The PLS-DA model was tested for overfitting using permutation tests and cross-validation analysis of variance (CV-ANOVA).

ACKNOWLEDGEMENTS

We thank our colleagues Roneel Prakash for technical assistance, Helen Boldingh and Trisha Pereira for carrying out starch measurements, Hilary Ireland for guidance with RNA extractions, Nitisha Bhargava and Alex Nguyen for advice with chlorophyll and anthocyanin measurements, and Nigel Gapper for critically reviewing the manuscript. Open access publishing facilitated by New Zealand Institute for Plant and Food Research Ltd, as part of the Wiley - New Zealand Institute for Plant and Food Research Ltd agreement via the Council of Australian University Librarians.

CONFLICT OF INTEREST

The authors declare no conflicts of interest.

AUTHOR CONTRIBUTIONS

KG obtained the physiological data. KG, RS, AN and EOD carried out biochemical, molecular and cell wall analyses. CD and LF analysed the transcriptomic data. ST and MD

made and cared for the transgenic plants. BK and MK conducted transpiration assays. RR and IH undertook the immunolabelling and microscopy. RS, RJS, MK, DB and RA designed the research, analysed the data and wrote the paper. This work was funded by the New Zealand Ministry of Business, Innovation and Employment and internal Plant & Food Research funding.

DATA AVAILABILITY STATEMENT

All relevant data can be found within the manuscript and its supporting materials.

SUPPORTING INFORMATION

Additional Supporting Information may be found in the online version of this article.

Table S1. Sugar composition of pectin-rich fractions in wildtype and PGox apple fruit.

Table S2. Partitioning of pectin-rich cell wall extracts in wildtype and PGox apple fruit.

Figure S1. Screening of PGox apple lines in leaves and fruit.

Figure S2. Weight, firmness, chlorophyll, and anthocyanin measurements of wildtype and PGox fruit.

Figure S3. Toluidine blue staining of wildtype and PGox fruit.

Figure S4. Cryo-SEM fractures of frozen apple tissue.

Figure S5. Size exclusion chromatography of polyuronides in water-soluble extracts in apple peel and cortex during development.

Figure S6. Size exclusion chromatography of polyuronides in CDTA-soluble extracts in apple peel and cortex during development.

Figure S7. Size exclusion chromatography of polyuronides in Na_2CO_3-soluble extracts in apple peel and cortex during development.

Figure S8. Degree of methyl esterification of cell wall material and CDTA-soluble pectin in apple peel and cortex during development.

Table S3. Differentially expressed genes in PGox3502 apple fruit at 60 and 100 DAP.

REFERENCES

Ahmed, A.E.R. & **Labavitch, J.M.** (1977) A simplified method for accurate determination of cell wall uronide content. *Journal of Food Biochemistry*, **1**, 361–365.

Albersheim, P., **Nevins, D.J.**, **English, P.D.** & **Karr, A.** (1967) A method for the analysis of sugars in plant cell-wall polysaccharides by gas-liquid chromatography. *Carbohydrate Research*, **5**, 340–345.

Ampomah-Dwamena, C., **Driedonks, N.**, **Lewis, D.**, **Shumskaya, M.**, **Chen, X.**, **Wurtzel, E.T.** ***et al.*** (2015) The phytoene synthase gene family of apple (*malus* x *domestica*) and its role in controlling fruit carotenoid content. *BMC Plant Biology*, **15**, 185.

Anders, S. (2010) Analysing RNA-seq data with the DESeq package. *Molecular Biology*, **43**, 1–17.

Anderson, C.T. & **Kieber, J.J.** (2020) Dynamic construction, perception, and remodeling of plant cell walls. *Annual Review of Plant Biology*, **71**, 39–69.

Atkinson, R.G. (1994) A cDNA clone for endopolygalacturonase gene from apple. *Plant Physiology*, **195**, 1437–1438.

Atkinson, R.G., **Schröder, R.**, **Hallett, I.C.**, **Cohen, D.** & **MacRae, E.A.** (2002) Overexpression of polygalacturonase in transgenic apple trees leads to a range of novel phenotypes involving changes in cell adhesion. *Plant Physiology*, **129**, 122–133.

Atkinson, R.G., **Sutherland, P.W.**, **Johnston, S.L.**, **Gunaseelan, K.**, **Hallett, I.C.**, **Mitra, D.** ***et al.*** (2012) Down-regulation of *POLYGALACTURONASE1* alters firmness, tensile strength and water loss in apple (*Malus* x *domestica*) fruit. *BMC Plant Biology*, **12**, 129.

Ban, Q.Y., **Han, Y.**, **He, Y.H.**, **Jin, M.J.**, **Han, S.K.**, **Suo, J.T.** ***et al.*** (2018) Functional characterization of persimmon β-galactosidase gene *DkGAL1* in tomato reveals cell wall modification related to fruit ripening and radicle elongation. *Plant Science*, **274**, 109–120.

Bhargava, N., **Ampomah-Dwamena, C.**, **Voogd, C.** & **Allan, A.C.** (2023) Comparative transcriptomic and plastid development analysis sheds light on the differential carotenoid accumulation in kiwifruit flesh. *Frontiers in Plant Science*, **14**, 1213086.

Blumenkrantz, N. & **Asboe-Hansen, G.** (1973) New method for quantitative determination of uronic acids. *Analytical Biochemistry*, **54**, 484–489.

Brummell, D.A. (2006) Cell wall disassembly in ripening fruit. *Functional Plant Biology*, **33**, 103–119.

Brummell, D.A. (2020) Sensing when the wall comes tumbling down. *Journal of Experimental Botany*, **71**, 6865–6868.

Brummell, D.A., **Bowen, J.K.** & **Gapper, N.E.** (2022) Biotechnological approaches for controlling postharvest fruit softening. *Current Opinion in Biotechnology*, **78**, 102786.

Brummell, D.A. & **Harpster, M.H.** (2001) Cell wall metabolism in fruit softening and quality and its manipulation in transgenic plants. *Plant Molecular Biology*, **47**, 311–340.

Brummell, D.A., **Harpster, M.H.**, **Civello, P.M.**, **Palys, J.M.**, **Bennett, A.B.** & **Dunsmuir, P.** (1999) Modification of expansin protein abundance in tomato fruit alters softening and cell wall polymer metabolism during ripening. *Plant Cell*, **11**, 2203–2216.

Chang, S., **Puryear, J.** & **Cairney, J.** (1993) A simple and efficient method for isolating RNA from pine trees. *Plant Molecular Biology Reporter*, **11**, 113–116.

Chen, S., **Zhou, Y.**, **Chen, Y.** & **Gu, J.** (2018) fastp: an ultra-fast all-in-one FASTQ preprocessor. *Bioinformatics*, **34**, i884–i890.

Chen, Y.-H., **Xie, B.**, **An, X.-H.**, **Ma, R.-P.**, **Zhao, D.-Y.**, **Cheng, C.-G.** ***et al.*** (2022) Overexpression of the apple expansin-like gene *MdEXLB1* accelerates the softening of fruit texture in tomato. *Journal of Integrative Agriculture*, **21**, 3578–3588.

Collins, P.P., **O'Donoghue, E.M.**, **Rebstock, R.**, **Tiffin, H.R.**, **Sutherland, P.W.**, **Schröder, R.** ***et al.*** (2019) Cell type-specific gene expression underpins remodelling of cell wall pectin in exocarp and cortex during apple fruit development. *Journal of Experimental Botany*, **21**, 6085–6099.

Costa, F., **Peace, C.P.**, **Stella, S.**, **Serra, S.**, **Musacchi, S.**, **Bazzani, M.** ***et al.*** (2010) QTL dynamics for fruit firmness and softening around an ethylene-dependent polygalacturonase gene in apple (*Malus x domestica* Borkh.). *Journal of Experimental Botany*, **61**, 3029–3039.

Daccord, N., **Celton, J.M.**, **Linsmith, G.**, **Becker, C.**, **Choisne, N.**, **Schijlen, E.** ***et al.*** (2017) High-quality *de novo* assembly of the apple genome and methylome dynamics of early fruit development. *Nature Genetics*, **49**, 1099–1106.

Du, J., **Anderson, C.T.** & **Xiao, C.** (2022) Dynamics of pectic homogalacturonan in cellular morphogenesis and adhesion, wall integrity sensing and plant development. *Nature Plants*, **8**, 332–340.

Espley, R.V., **Hellens, R.P.**, **Putterill, J.**, **Stevenson, D.E.**, **Kutty-Amma, S.** & **Allan, A.C.** (2007) Red colouration in apple fruit is due to the activity of the MYB transcription factor, MdMYB10. *The Plant Journal*, **49**, 414–427.

Espley, R.V., **Leif, D.**, **Plunkett, B.**, **McGhie, T.**, **Henry-Kirk, R.**, **Hall, M.** ***et al.*** (2019) Red to brown: An elevated anthocyanic response in apple drives ethylene to advance maturity and fruit flesh browning. *Frontiers in Plant Science*, **10**, 1248.

Ferrari, S., **Savatin, D.V.**, **Sicilia, F.**, **Gramegna, G.**, **Cervone, F.** & **Lorenzo, G.D.** (2013) Oligogalacturonides: plant damage-associated molecular patterns and regulators of growth and development. *Frontiers in Plant Science*, **4**, 49.

Fullerton, C.G., **Prakash, R.**, **Ninan, A.S.**, **Atkinson, R.G.**, **Hallett, I.C.**, **Schaffer, R.J.** ***et al.*** (2020) Fruit from two kiwifruit genotypes with contrasting softening rates show differences in the xyloglucan and pectin domains of the cell wall. *Frontiers in Plant Science*, **11**, 964.

Geyer, U. & **Schönherr, J.** (1988) *In vitro test for effects of surfactants and formulations on permeability of plant cuticles*, Vol. **371**. Washington, DC: ACS Publications, pp. 22–33.

Giovannoni, J. (2001) Molecular biology of fruit maturation and ripening. *Annual Review of Plant Physiology and Plant Molecular Biology*, **52**, 725–749.

Han, Y., **Ban, Q.**, **Li, H.**, **Hou, Y.**, **Jin, M.**, **Han, S.** ***et al.*** (2016) DkXTH8, a novel xyloglucan endotransglucosylase/hydrolase in persimmon, alters cell wall structure and promotes leaf senescence and fruit postharvest softening. *Scientific Reports*, **6**, 39155.

He, Y., **Karre, S.**, **Johal, G.S.**, **Christensen, S.A.** & **Balint-Kurti, P.** (2019) A maize polygalacturonase functions as a suppressor of programmed cell death in plants. *BMC Plant Biology*, **19**, 310.

Huang, D.W., **Sherman, B.T.** & **Lempicki, R.A.** (2009) Systematic and integrative analysis of large gene lists using DAVID bioinformatics resources. *Nature Protocols*, **4**, 44–57.

Janssen, B.J., **Thodey, K.**, **Schaffer, R.J.**, **Alba, R.**, **Balakrishnan, L.**, **Bishop, R.** ***et al.*** (2008) Global gene expression analysis of apple fruit development from the floral bud to ripe fruit. *BMC Plant Biology*, **8**, 16.

Jia, K.A., **Wang, W.**, **Zhang, Q.** & **Jia, W.S.** (2023) Cell wall integrity signaling in fruit ripening. *International Journal of Molecular Sciences*, **24**, 4054.

Jiang, F., **Lopez, A.**, **Jeon, S.**, **de Freitas, S.T.**, **Yu, Q.**, **Wu, Z.** ***et al.*** (2019) Disassembly of the fruit cell wall by the ripening-associated polygalacturonase and expansin influences tomato cracking. *Horticulture Research*, **6**, 17.

Johnston, J.W., **Gunaseelan, K.**, **Pidakala, P.**, **Wang, M.** & **Schaffer, R.J.** (2009) Co-ordination of early and late ripening events in apples is regulated through differential sensitivities to ethylene. *Journal of Experimental Botany*, **60**, 2689–2699.

Jung, S., **Lee, T.**, **Cheng, C.H.**, **Buble, K.**, **Zheng, P.**, **Yu, J.** ***et al.*** (2019) 15 years of GDR: new data and functionality in the genome database for Rosaceae. *Nucleic Acids Research*, **47**, D1137–D1145.

Khanal, B.P. & **Knoche, M.** (2014) Mechanical properties of apple skin are determined by epidermis and hypodermis. *Journal of the American Society for Horticultural Science*, **139**, 139–147.

Khanal, B.P., **Si, Y.** & **Knoche, M.** (2020) Lenticels and apple fruit transpiration. *Postharvest Biology and Technology*, **167**, 111221.

Kim, D., **Paggi, J.M.**, **Park, C.**, **Bennett, C.** & **Salzberg, S.L.** (2019) Graph-based genome alignment and genotyping with HISAT2 and HISAT-genotype. *Nature Biotechnology*, **37**, 907–915.

Kingston, C.M. (1992) Maturity indices for apple and pear. *Horticultural Reviews*, **13**, 407–432.

Knoche, M. & **Lang, A.** (2017) Ongoing growth challenges fruit skin integrity. *Critical Reviews in Plant Sciences*, **36**, 190–215.

Knoche, M., **Peschel, S.**, **Hinz, M.** & **Bukovac, M.J.** (2000) Studies on water transport through the sweet cherry fruit surface: characterizing conductance of the cuticular membrane using pericarp segments. *Planta*, **212**, 127–135.

Li, H., **Handsaker, B.**, **Wysoker, A.**, **Fennell, T.**, **Ruan, J.**, **Homer, N.** ***et al.*** (2009) The sequence alignment/map format and SAMtools. *Bioinformatics*, **25**, 2078–2079.

Li, W.X., **He, C.**, **Wei, H.L.**, **Qian, J.K.**, **Xie, J.N.**, **Li, Z.Q.** ***et al.*** (2023) *VvPL11* is a key member of the pectin lyase gene family involved in grape softening. *Horticulturae*, **9**, 182.

Liu, H., **Qian, M.**, **Song, C.**, **Li, J.**, **Zhao, C.**, **Li, G.** ***et al.*** (2018) Down-regulation of *PpBGAL10* and *PpBGAL16* delays fruit softening in peach by reducing polygalacturonase and pectin methylesterase activity. *Frontiers in Plant Science*, **9**, 1015.

Longhi, S., **Hamblin, M.T.**, **Trainotti, L.**, **Peace, C.P.**, **Velasco, R.** & **Costa, F.** (2013) A candidate gene based approach validates *Md-PG1* as the main responsible for a QTL impacting fruit texture in apple (*Malus* x *domestica Borkh*). *BMC Plant Biology*, **13**, 37.

Ma, Y., **Zhou, L.**, **Wang, Z.**, **Chen, J.** & **Qu, G.** (2016) Oligogalacturonic acids promote tomato fruit ripening through the regulation of 1-aminocyclopropane-1-carboxylic acid synthesis at the transcriptional and post-translational levels. *BMC Plant Biology*, **16**, 13.

Maguire, K.M., **Lang, A.**, **Banks, N.H.**, **Hall, A.**, **Hopcroft, D.** & **Bennett, R.** (1999) Relationship between water vapour permeance of apples and microcracking of the cuticle. *Postharvest Biology and Technology*, **17**, 89–96.

Martin, L.B. & **Rose, J.K.** (2014) There's more than one way to skin a fruit: formation and functions of fruit cuticles. *Journal of Experimental Botany*, **65**, 4639–4651.

Migicovsky, Z., **Yeats, T.H.**, **Watts, S.**, **Song, J.**, **Forney, C.F.**, **Burgher-MacLellan, K.** ***et al.*** (2021) Apple ripening is controlled by a NAC transcription factor. *Frontiers in Genetics*, **12**, 671300.

Moctezuma, E., **Smith, D.L.** & **Gross, K.C.** (2003) Antisense suppression of a β-galactosidase gene (*TBG6*) in tomato increases fruit cracking. *Journal of Experimental Botany*, **54**, 2025–2033.

Ng, J.K., **Schroder, R.**, **Brummell, D.A.**, **Sutherland, P.W.**, **Hallett, I.C.**, **Smith, B.G.** ***et al.*** (2015) Lower cell wall pectin solubilisation and galactose loss during early fruit development in apple (*Malus* x *domestica*) cultivar 'Scifresh' are associated with slower softening rate. *Journal of Plant Physiology*, **176**, 129–137.

Ng, J.K.T., **Schröder, R.**, **Sutherland, P.W.**, **Hallett, I.C.**, **Hall, M.I.**, **Prakash, R.** ***et al.*** (2013) Cell wall structures leading to cultivar differences in softening rates develop early during apple (*Malus* x *domestica*) fruit growth. *BMC Plant Biology*, **13**, 183.

Ohara, T., **Takeuchi, H.**, **Sato, J.**, **Nakamura, A.**, **Ichikawa, H.**, **Yokoyama, R.** ***et al.*** (2021) Structural alteration of rice pectin affects cell wall mechanical strength and pathogenicity of the rice blast fungus under weak light conditions. *Plant & Cell Physiology*, **62**, 641–649.

Paniagua, A.C., **East, A.R.**, **Hindmarsh, J.P.** & **Heyes, J.A.** (2013) Moisture loss is the major cause of firmness change during postharvest storage of blueberry. *Postharvest Biology and Technology*, **79**, 13–19.

Paniagua, C., **Ric-Varas, P.**, **Garcia-Gago, J.A.**, **Lopez-Casado, G.**, **Blanco-Portales, R.**, **Munoz-Blanco, J.** ***et al.*** (2020) Elucidating the role of polygalacturonase genes in strawberry fruit softening. *Journal of Experimental Botany*, **71**, 7103–7117.

Peschel, S. & **Knoche, M.** (2005) Characterization of microcracks in the cuticle of developing sweet cherry fruit. *Journal of the American Society for Horticultural Science*, **130**, 487–495.

Prakash, R., **Hallett, I.C.**, **Wong, S.F.**, **Johnston, S.L.**, **O'Donoghue, E.M.**, **McAtee, P.A.** ***et al.*** (2017) Cell separation in kiwifruit without development of a specialised detachment zone. *BMC Plant Biology*, **17**, 86.

Reynoud, N., **Geneix, N.**, **Petit, J.**, **D'Orlando, A.**, **Fanuel, M.**, **Marion, D.** ***et al.*** (2022) The cutin polymer matrix undergoes a fine architectural tuning from early tomato fruit development to ripening. *Plant Physiology*, **190**, 1821–1840.

Rui, Y., **Xiao, C.**, **Yi, H.**, **Kandemir, B.**, **Wang, J.Z.**, **Puri, V.M.** ***et al.*** (2017) POLYGALACTURONASE INVOLVED IN EXPANSION3 functions in seedling development, rosette growth, and stomatal dynamics in *Arabidopsis thaliana*. *Plant Cell*, **29**, 2413–2432.

Saladié, M., **Matas, A.J.**, **Isaacson, T.**, **Jenks, M.A.**, **Goodwin, S.M.**, **Niklas, K.J.** ***et al.*** (2007) A reevaluation of the key factors that influence tomato fruit softening and integrity. *Plant Physiology*, **144**, 1012–1028.

Schaffer, R.J., **Friel, E.N.**, **Souleyre, E.J.F.**, **Bolitho, K.**, **Thodey, K.**, **Ledger, S.** ***et al.*** (2007) A genomics approach reveals that aroma production in apple is controlled by ethylene predominantly at the final step in each biosynthetic pathway. *Plant Physiology*, **144**, 1899–1912.

Shackel, K.A., **Greve, C.**, **Labavitch, J.M.** & **Ahmadi, H.** (1991) Cell turgor changes associated with ripening in tomato pericarp tissue. *Plant Physiology*, **97**, 814–816.

Shi, Y., **Li, B.J.**, **Grierson, D.** & **Chen, K.S.** (2023) Insights into cell wall changes during fruit softening from transgenic and naturally occurring mutants. *Plant Physiology*, **192**, 1671–1683.

Simpson, S.D., **Ashford, D.A.**, **Harvey, D.J.** & **Bowles, D.J.** (1998) Short chain oligogalacturonides induce ethylene production and expression of the gene encoding aminocyclopropane 1-carboxylic acid oxidase in tomato plants. *Glycobiology*, **8**, 579–583.

Sitrit, Y. & **Bennett, A.B.** (1998) Regulation of tomato fruit polygalacturonase mRNA accumulation by ethylene: a re-examination. *Plant Physiology*, **116**, 1145–1150.

Smith, G.S., **Clark, C.J.** & **Boldingh, H.L.** (1992) Seasonal accumulation of starch by components of the kiwifruit vine. *Annals of Botany*, **70**, 19–25.

Sutherland, P., **Hallett, I.** & **Jones, M.** (2009) Probing cell wall structure and development by the use of antibodies: a personal perspective. *The New Zealand Journal of Forestry Science*, **39**, 197–205.

Tacken, E., **Ireland, H.**, **Gunaseelan, K.**, **Karunairetnam, S.**, **Wang, D.**, **Schultz, K.** ***et al.*** (2010) The role of ethylene and cold temperature in the regulation of the apple POLYGALACTURONASE 1 gene and fruit softening. *Plant Physiology*, **153**, 294–305.

Veraverbeke, E.A., **Verboven, P.**, **Van Oostveldt, P.** & **Nicolaí, B.M.** (2003a) Prediction of moisture loss across the cuticle of apple (*Malus sylvestris* subsp. *mitis* (Wallr.)) during storage: part 1. Model development and determination of diffusion coefficients. *Postharvest Biology and Technology*, **30**, 75–88.

Veraverbeke, E.A., **Verboven, P.**, **Van Oostveldt, P.** & **Nicolaí, B.M.** (2003b) Prediction of moisture loss across the cuticle of apple (*Malus sylvestris*

subsp. *mitis* (Wallr.)) during storage: part 2. Model simulations and practical applications. *Postharvest Biology and Technology*, **30**, 89–97.

Wada, H., **Shackel, K.A.** & **Matthews, M.A.** (2008) Fruit ripening in *Vitis vinifera*: apoplastic solute accumulation accounts for pre-veraison turgor loss in berries. *Planta*, **227**, 1351–1361.

Wang, D., **Yeats, T.H.**, **Uluisik, S.**, **Rose, J.K.C.** & **Seymour, G.B.** (2018) Fruit softening: revisiting the role of pectin. *Trends in Plant Science*, **23**, 302–310.

Witasari, L.D., **Huang, F.C.**, **Hoffmann, T.**, **Rozhon, W.**, **Fry, S.C.** & **Schwab, W.** (2019) Higher expression of the strawberry xyloglucan endotransglucosylase/hydrolase genes *FvXTH9* and *FvXTH6* accelerates fruit ripening. *The Plant Journal*, **100**, 1237–1253.

Wolf, S. (2022) Cell wall signaling in plant development and defense. *Annual Review of Plant Biology*, **73**, 323–353.

Woolf, A.B., **Wibisono, R.**, **Farr, J.**, **Hallett, I.**, **Richter, L.**, **Oey, I.** ***et al.*** (2013) Effect of high pressure processing on avocado slices. *Innovative Food Science and Emerging Technologies*, **18**, 65–73.

Wu, Q., **Szakáca-Dobozi, M.**, **Hemmat, M.** & **Hrazdina, G.** (1993) Endopolygalacturonase in apples (*Malus domestica*) and its expression during fruit ripening. *Plant Physiology*, **102**, 219–225.

Xiao, C., **Somerville, C.** & **Anderson, C.T.** (2014) POLYGALACTURONASE INVOLVED IN EXPANSION1 functions in cell elongation and flower development in *Arabidopsis*. *Plant Cell*, **26**, 1018–1035.

Xue, C., **Guan, S.C.**, **Chen, J.Q.**, **Wen, C.J.**, **Cai, J.F.** & **Chen, X.** (2020) Genome wide identification and functional characterization of strawberry pectin methylesterases related to fruit softening. *BMC Plant Biology*, **20**, 13.

Yang, L., **Cong, P.**, **He, J.**, **Bu, H.**, **Qin, S.** & **Lyu, D.** (2022) Differential pulp cell wall structures lead to diverse fruit textures in apple (*Malus domestica*). *Protoplasma*, **259**, 1205–1217.

Yang, L., **Huang, W.**, **Xiong, F.**, **Xian, Z.**, **Su, D.**, **Ren, M.** ***et al.*** (2017) Silencing of *SlPL*, which encodes a pectate lyase in tomato, confers enhanced fruit firmness, prolonged shelf-life and reduced susceptibility to grey mould. *Plant Biotechnology Journal*, **15**, 1544–1555.

Yao, J.L., **Cohen, D.**, **Atkinson, R.**, **Richardson, K.** & **Morris, B.** (1995) Regeneration of transgenic plants from the commercial apple cultivar Royal Gala. *Plant Cell Reports*, **14**, 407–412.

Yauk, Y.-K., **Chagné, D.**, **Tomes, S.**, **Matich, A.J.**, **Wang, M.Y.**, **Chen, X.** ***et al.*** (2015) The *O*-methyltransferase gene *MdoOMT1* is required for biosynthesis of methylated phenylpropenes in ripe apple fruit. *The Plant Journal*, **82**, 937–950.

Yu, J., **Wang, R.**, **Ma, W.**, **Lei, S.**, **Zhu, M.** & **Yang, G.** (2023) Pectate lyase gene *VvPL1* plays a role in fruit cracking of table grapes. *Journal of Agricultural and Food Chemistry*, **71**, 1643–1654.

Zamil, M.S. & **Geitmann, A.** (2017) The middle lamella - more than a glue. *Physical Biology*, **14**, 015004.